The University of British Columbia

FACULTY OF GRADUATE STUDIES

PROGRAMME OF THE

FINAL ORAL EXAMINATION

FOR THE DEGREE OF

DOCTOR OF PHILOSOPHY

of

R.L. Pike

B.Sc., The University of British Columbia

IN ROOM 301, HENNINGS BUILDING

WEDNESDAY, SEPTEMBER 20, 1967, AT 3:30 P.M.

COMMITTEE IN CHARGE

Chairman: B. N. Moyls

B. Ahlborn
J.W. Bichard
R.W. Burling
A. Folkierski
R.M. Ellis
R. Nodwell
C.F. Schwerdtfeger

External Examiner: V.R. Malkus
Woods Hole Oceanographic Institution,
Woods Hole, Massachusetts.

Research Supervisor: F.L. Curzon

INVESTIGATION OF FLUID SURFACE WAVES WITH A NEW MICROWAVE RESONANCE TECHNIQUE

ABSTRACT

A new microwave technique has been developed for the experimental study of small amplitude surface waves on an electrically conducting fluid. The fluid forms one of the walls of a resonating, microwave cavity. Surface waves with amplitudes as small as 10^{-3} cm. can be measured by observing the resulting change in the resonant frequency of the cavity.

This technique has been successfully used to measure the viscous and magnetic damping coefficient of a small amplitude, standing, surface wave in liquid mercury. The magnetic damping coefficient for a vertical, magnetic field was found to be in good agreement with a calculation that was made for low magnetic Reynolds numbers. When the viscous damping coefficient was compared with the standard theory, which allows horizontal motion of the surface, a disagreement of up to a factor of four was found.

It, however, showed excellent agreement with a modified theory which assumes that there is no horizontal motion of the surface.

GRADUATE STUDIES

Field of Study: Plasma Physics

Applied Electronics	M. Kharadly
Elementary Quantum Mechanics	G.M. Volkoff
Waves	R.M. Ellis
Electromagnetic Theory	P. Rastall
Plasma Dynamics	F.L. Curzon
Plasma Physics	L. Sobrino
Analysis of Linear Systems	E.V. Bohn
Theory of Ideal Fluids	G.V. Parkinson
Advanced Plasma Physics	R. Nodwell

AWARDS

1960-64	B. C. Government Scholarships
1965-67	National Research Council Scholarships
1967	National Research Council Postdoctorate Fellowship

INVESTIGATION OF FLUID SURFACE WAVES WITH A NEW MICROWAVE RESONANCE TECHNIQUE

by

Robert L. Pike

B.Sc. University of British Columbia, 1964

A THESIS SUBMITTED IN PARTIAL FULFILMENT OF THE REQUIREMENTS FOR THE DEGREE OF

DOCTORATE OF PHILOSOPHY

in the department

of

PHYSICS

We accept this thesis as conforming to the required standard

THE UNIVERSITY OF BRITISH COLUMBIA

AUGUST, 1967

In presenting this thesis in partial fulfilment of the requirements for an advanced degree at the University of British Columbia, I agree that the Library shall make it freely available for reference and Study. I further agree that permission for extensive copying of this thesis for scholarly purposes may be granted by the Head of my Department or by his representatives. It is understood that copying or publication of this thesis for financial gain shall not be allowed without my written permission.

Department of Physics

The University of British Columbia
Vancouver 8, Canada

Date Sept 22 1967

ABSTRACT

A new microwave technique has been developed for the experimental study of small amplitude surface waves on an electrically conducting fluid. The fluid forms one of the walls of a resonating, microwave cavity. Surface waves with amplitudes as small as 10^{-3} cm. can be measured by observing the resulting change in the resonant frequency of the cavity.

This technique has been successfully used to measure the viscous and magnetic damping coefficient of a small amplitude, standing, surface wave in liquid mercury. The magnetic damping coefficient (for a vertical, magnetic field) was found to be in good agreement with a calculation that was made for low magnetic Reynolds numbers. When the viscous damping coefficient was compared with the standard theory, which allows horizontal motion of the surface, a disagreement of up to a factor of four was found. It, however, showed excellent agreement with a modified theory which assumes that there is no horizontal motion of the surface.

TABLE OF CONTENTS

APPENDICES

LIST OF ILLUSTRATIONS

TABLES

ACKNOWLEDGEMENTS

I wish to thank Dr. F. L. Curzon for the excellent supervision I received while carrying out this investigation.

The assistance of Mr. W. Ratzlaff and Mr. J. Dooyeweerd in the field of electronics and the assistance of Mr. R. Ninnis, Mr. W. Morrison, Mr. D. Stonebridge, and other members of the technical staff in the construction of the apparatus is gratefully acknowledged. Helpful information and suggestions by members of the plasma group and members of my Ph. D. committee are also gratefully acknowledged.

I wish to thank the National Research Council of Canada for financial assistance during the course of this work.

Chapter 1 INTRODUCTION

Surface waves are studied in many scientific fields: oceanography, geophysics, plasma physics, etc. They are of interest to the plasma physicist with respect to the confinment of plasmas. All plasmas in one way or another must have surfaces to be separated from our normal, hostile room temperature environment. These surfaces, produced under the influence of gravitational and magnetic fields, tend to become unstable or distorted. This distortion can be described by a series of sine and cosine waves. Hence, the study of a plasma surface involves the study of surface waves. The effect of gravitational and magnetic fields on the surface motion is of great interest. The study of this effect is complicated, however, by temperature and mass density gradients which are present in most laboratory plasmas. The effect can be computed and observed more easily if an electrically conducting fluid, such as mercury, is used instead of a plasma. For this reason a theoretical and an experimental study of surface waves on an electrically conducting fluid have been made.

The time dependence for a linear (small amplitude) surface wave is usually expressed in the form $\exp(\sigma t)\cos(2\pi f t)$. σ is called the damping coefficient and f is called the oscillation frequency of the surface wave. It was the aim of this thesis to study the damping coefficient of a surface wave under the influence of a magnetic field, but it was found necessary, first, to investigate the damping of a surface wave free of magnetic fields and to consider the methods used to measure this wave.

It was found that the linear theory of surface waves has not previously been properly tested and verified in many cases (ref. 18). This is at least partly due to the problems associated with the wave guages used in the past. Devices such as capacitance (ref. 41) and resistance (ref. 42 and 43) wave guages are available to study surface waves. They, however, suffer from the

difficulties common to all immersion devices. The difficulties are attributable to:

(1) the erratic dynamic behaviour of the meniscus,

(2) the existence of a viscous film of fluid on the gauge as the free surface recedes,

and (3) large disturbances around the gauge when fluid velocities are large (e.g. the upward directed jet at the stagnation point and caviation in the wake).

Also, the usefulness of these and other devices is limited, in many cases, by the lack of the sensitivity required to study linear surface waves. For example, the linearity restriction, $\zeta_o K << (HK)^3$, (where ζ_o is the wave amplitude, K is the wave number and H is the fluid depth) requires that $\zeta_o K \leq 10^{-4}$ for shallow fluid ($KH \simeq 0.1$) experiments. Investigation of shallow fluid surface waves, as a result, has been restricted because reliable methods of measuring ζ_o when $K\zeta_o \leq 10^{-4}$ have not been available.

In view of these problems Curzon and Howard (ref. 39 and 40) developed theoretically a new technique to study linear surface waves on a column of an electrically conducting fluid. The essential idea behind this technique is the following. If an electrically conducting fluid acts as a wall of a microwave cavity, any change in shape of that fluid (e.g. surface waves) causes a change in the shape of the cavity which, in turn, causes a change in the resonant frequency of that cavity. It is, therefore, possible to monitor the motion of the fluid by monitoring the change in the resonant frequency of the microwave cavity. This idea was adopted by the author to develop theoretically and experimentally a new technique to study surface waves on a flat surface.

In chapter 2 Slater's theorem (ref. 2) is used to calculate the change in frequency of a microwave cavity from ω to ω_a when a surface wave of

amplitude ζ_0 is set up on the end plate of the cavity of length L. Results show that $\frac{(\omega_a - \omega)}{\omega \zeta_0} L \leq 1$. There are two important features here. First, the change in the resonant frequency is directly proportional to the surface wave amplitude. This will make the observation of the time dependence of ζ_0 very easy. Secondly, the system is sensitive to small amplitude surface waves. Since values of 0.5×10^{-4} for $\frac{\omega_a - \omega}{\omega}$ are easily observed it appears that surface waves such that $\zeta_0 k \leq 0.5 \times 10^{-4}$ can be detected. This technique, therefore, can be used to study linear surface waves, even in the shallow fluid region. Another interesting feature is also found. Calculations show that a rectangular cavity when used to study surface waves acts as an automatic Fourier analyser. It appears that a rectangular cavity can be constructed so the change in resonant frequency of the cavity is directly proportional to only one Fourier component of the surface wave under investigation. This feature should eliminate the tedious and complex procedure of Fourier analysing arbitrary surface waves. These features, together with the fact that the system is free of the problems associated with immersion devices, make the microwave cavity a useful diagnostic tool for studying surface waves.

A cylindrical microwave cavity has been used to measure the oscillation frequency, f, and viscous damping coefficient, σ_0, of a standing, axisymmetric wave in shallow and deep pools of mercury. This work, described in chapters 3, 4 and 5, shows that the observed oscillation frequencies are higher than predicted by theory by up to 15%. The results indicate that the meniscus is the cause of this discrepancy. The observed viscous damping coefficients are higher than predicted by the standard theory of Case and Parkinson (ref. 7) by up to 400%. In view of this discrepancy the assumption that there is no horizontal motion of the surface is introduced.

According to Lamb and Levich (ref. 21 and 22) this is the condition that must be used when an incompressible, insoluble, surface film is present. The author calculated that the additional viscous damping coefficient resulting from the above assumption is equal to $-\sqrt{\frac{\nu 2\pi f}{2}} \frac{K \cosh^2(KH)}{\sinh(2KH)}$. ν is the kinematic viscosity of the fluid. The experimental results are found to be in excellent agreement with the theory when this effect is included. It is, therefore, concluded that there was no horizontal, surface motion. It is suggested that this was due to the presence of a surface film. Since the literature indicates that surface films are present on fluids in ordinary laboratory experiments, the above calculation should be useful to those studying surface waves.

The study of magnetohydrodynamic surface waves is initiated by the author's calculation of the magnetic damping coefficient, σ_B, for low magnetic Reynolds numbers. It is calculated in chapter 6 for an axisymmetric, linear, standing, surface wave on an incompressible, ideal fluid with a finite electrical conductivity, q, and mass density, ρ. The effect of a vertical constant, applied, uniform, magnetic field, B_3, is considered. Detailed calculations are made for the case $\frac{q B_3^2}{\rho 2\pi f} \ll 1$. The calculations show that the oscillation frequency is independent of B_3 and that σ_B is given by $\sigma_B = -\frac{q B_3^2}{4\rho} \left\{ 1 + \frac{4KH}{\exp(2KH) - \exp(-2KH)} \right\}$. This calculation is experimentally verified by a series of experiments with liquid mercury. Chapter 7 describes this work. The magnetic damping coefficient, σ_B, is measured by measuring the total damping coefficient, σ, and assuming that $\sigma = \sigma_0 + \sigma_B$. Experimental results confirm this assumption. In agreement with the theory σ_B is found to be proportional to $\frac{q B_3^2}{2\rho}$ and to vary from

$-\frac{B_3^2 q}{2\rho\beta}$ (for $KH \leq 0.3$) to $-\frac{B_3^2 q}{4\rho\beta}$ (for $KH \geq 3.0$) as the fluid depth, H, is varied from small to large values. The rate at which σ_B varies with fluid depth is found to increase with K as predicted. All experimental values are within 10% of the theoretical values. This percentage is less than the maximum systematic percent error. These results, therefore, are considered to be in excellent agreement with our theory for the damping of surface waves in a vertical, magnetic field.

Chapter 2 MICROWAVE THEORY

The theory for the proposal to use a microwave cavity to study surface waves is developed in this chapter. Slater's theorem relating the change in the resonant frequency of a microwave cavity to small changes in shape of that cavity is given. His theorem is used to calculate frequency shifts for a surface wave perturbation of the cavity.

Section 1 SLATER'S THEOREM

Slater's theorem (ref. 2) describes the relation between the change in shape of a microwave cavity, the electromagnetic field distribution in that cavity, and the resulting change in resonant frequency of that cavity. The theorem is stated as: $\omega_a^2 = \omega^2 \left(1 + \iiint_{V_p} (Ba^2 - Ea^2)\, dv\right)$. (1.1.1)

ω is the resonant frequency of the cavity before its shape is changed.

ω_a is the resonant frequency of the cavity after its shape is changed.

Ba and Ea are given by $Ba^2 = |\hat{B}|^2/N_B^2$ $\quad Ea^2 = |\hat{E}|^2/N_E^2$

$N_B^2 = \iiint_{vc} |\hat{B}|^2\, dv$ and $N_E^2 = \iiint_{vc} |\hat{E}|^2\, dv$.

V_p is the change in volume of the cavity.

V_c is the original volume of the cavity.

$\hat{E}$ and $\hat{B}$ are the original electric and magnetic fields in the cavity.

It should be noted here that a perturbation method was used to develop this theorem. It was assumed that changing the cavity volume by the amount V_p causes only a small change in $\hat{E}$ and $\hat{B}$.

It is evident that the theory of resonant cavities must be considered before this theorem can be used.

Section 2 CAVITY RESONATORS

A microwave cavity is a container made of a material of high, electrical conductivity. The following definitions are made:

μ is the magnetic permeability in the cavity.

ϵ is the electric permittivity in the cavity.

ϵ_w is the electric permittivity in the cavity walls.

σ_c is the electrical conductivity in the cavity.

σ_w is the electrical conductivity in the cavity walls.

ω is the oscillation frequency of the electromagnetic (em.) wave in the cavity.

It is assumedthat:

(i) The material in the cavity and in the cavity walls is homogeneous and isotropic.

(ii) There is no free charge present.

(iii) The depth of penetration of the fields, the skin depth, in the cavity is very much larger than the wavelength of the fields and the skin depth in the cavity walls is very much smaller than the wavelength

(i.e. $\sigma_c/2\epsilon\omega \ll 1$ and $\sigma_w/2\epsilon_w\omega \gg 1$).

The nature of the e.m. field in the cavity is found by solving Maxwell's equations using the above assumptions. The solution for a cylindrical cavity can be found in most texts on electromagnetics (ref. 1). It will be stated here without proof. Figure 1 shows the geometry of the cavity.

There are two situations possible. First, the magnetic field in the cavity can be transverse to the axis of the cavity. This is called a transverse magnetic or T.M. mode. Secondly, the electric field can be transverse to the axis of the cavity. This is called a transverse electric

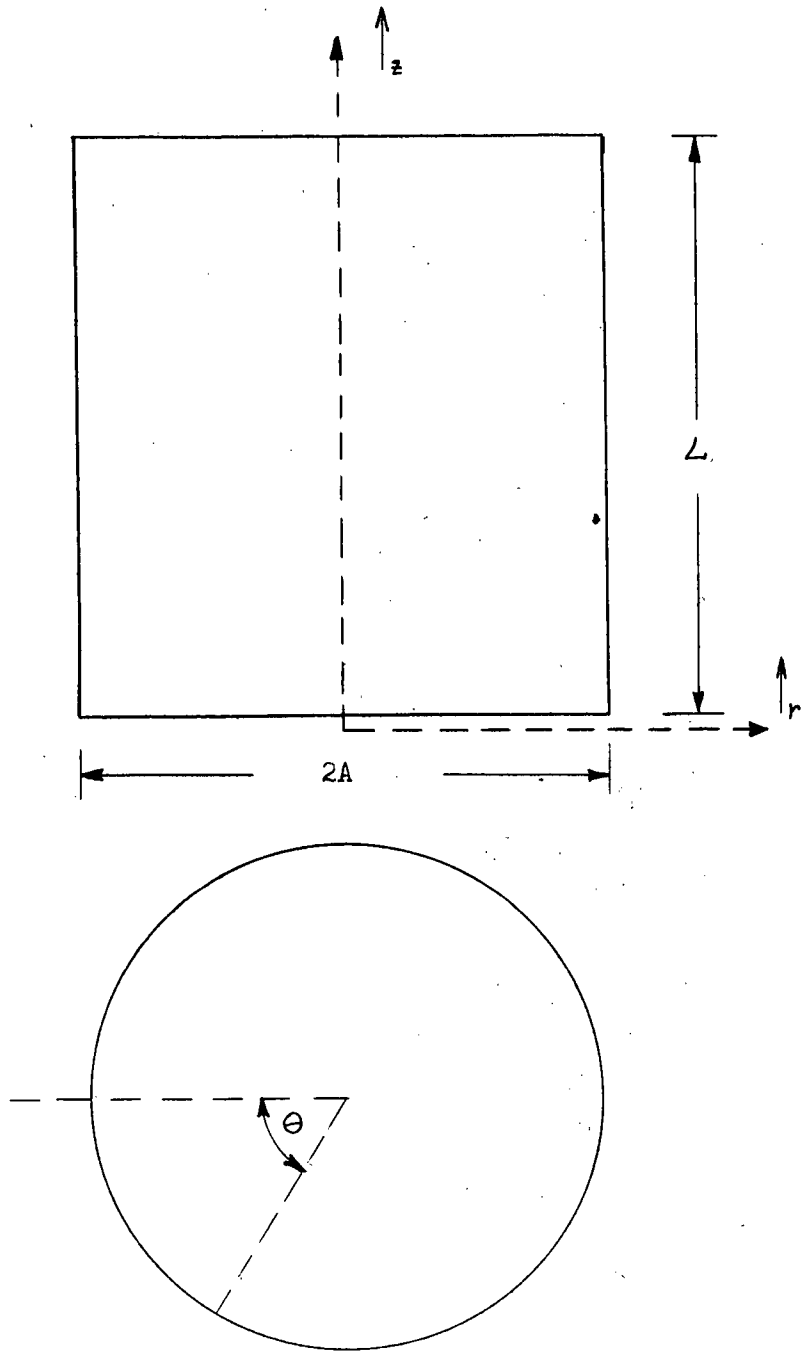

Figure I Cylindrical microwave cavity

or T. E. mode.

For the T. M. modes it can be shown that

$$\hat{B} = (B_\theta \hat{i}_\theta + B_r \hat{i}_r)e^{j\omega t} \quad \text{AND} \quad \hat{E} = (E_\theta \hat{i}_\theta + E_r \hat{i}_r + E_z \hat{i}_z)e^{j\omega t}$$

where
$$B_\theta = K_o J_\ell'(K_o r)\cos(\ell\theta)\cos(n\pi z/L)$$
$$B_r = \ell \frac{J_\ell}{r}(K_o r)\sin(\ell\theta)\cos(n\pi z/L)$$
$$E_\theta = -j\omega \frac{\ell n\pi}{k^2 r L} J_\ell(K_o r)\sin(\ell\theta)\sin(n\pi z/L)$$
$$E_r = j\omega \frac{n\pi K_o}{k^2 L} J_\ell'(K_o r)\cos(\ell\theta)\sin(n\pi z/L)$$
$$E_z = -\frac{j\omega K_o^2}{k^2} J_\ell(K_o r)\cos(\ell\theta)\cos(n\pi z/L)$$
$$k^2 = \omega^2 \epsilon\mu$$
$$J_\ell(K_o(\ell,m)A) = 0 \quad \text{-----}$$

(1.2.1)

J_ℓ is a Bessel function of order ℓ

and $j = \sqrt{-1}$.

Also, these standing em. waves are set up in the cavity only when

$$\omega^2 = \frac{K_o^2 + (n\pi/L)^2}{\epsilon\mu}. \qquad (1.2.2)$$

ω is the resonant frequency of the cavity and the three variables 1, m and n are integers which describe the azimuthal, radial and axial dependence, respectively, of the em. fields in the cavity. A specific T. M. mode is usually denoted by $T.M_{\ell,m,n}$.

Similarly for the T.E. 1, m, n, it can be shown that

$$\hat{B} = (B_\theta \hat{i}_\theta + B_r \hat{i}_r + B_z \hat{i}_z)e^{j\omega t} \text{ and } \hat{E} = (E_\theta \hat{i}_\theta + E_r \hat{i}_r)e^{j\omega t} \qquad (1.2.3)$$

where
$$B_\theta = -\frac{\pi\ell n J_\ell(Kr)}{rLK^2}\sin(\ell\theta)\cos(n\pi z/L)$$
$$B_r = \frac{n\pi}{LK} J_\ell'(Kr)\cos(\ell\theta)\cos(n\pi z/L)$$
$$B_z = J_\ell(Kr)\cos(\ell\theta)\sin(n\pi z/L)$$
$$E_\theta = -\frac{j\omega}{K} J_\ell'(Kr)\cos(\ell\theta)\sin(n\pi z/L)$$
$$E_r = -j\frac{\ell\omega}{rK^2} J_\ell(Kr)\sin(\ell\theta)\sin(n\pi z/L)$$

$$k^2 = \omega^2 \epsilon \mu$$

$$J_\ell' (K(l, m) A) = 0$$

and where

$$\omega^2 = \frac{K^2 + (n\pi/L)^2}{\epsilon \mu}. \qquad (1.2.4)$$

In the above equations for $\hat{B}$ and $\hat{E}$ a constant amplitude factor has been omitted. This factor is determined by the output power of the microwave system and is unimportant in the following calculations. Slater's theorem can now be used to compute the change in resonant frequency of a cavity for a surface wave perturbation of that cavity.

Section 3 CALCULATION OF THE RESONANT FREQUENCY CHANGE FOR A SURFACE WAVE IN A CYLINDRICAL CAVITY

The surface wave is assumed to be on the end plate (at $Z = 0$) of the cavity. In reference 6 it is shown that the amplitude of a linear, standing, surface wave in an incompressible fluid with small viscosity in a cylindrical basin can be expressed by

$$\zeta = \sum_{S,P} \zeta_o(S, P) \; J_S (K(S, P) r) \cos(S\theta) \text{ where } J_S' (K(S, P) A) = 0.$$

The calculation for $\frac{\omega_a - \omega}{\omega}$ will be made for a simple wave ($\zeta = \zeta_o J_S (Kr) \cos(S\theta)$). It is assumed that $n\pi\zeta_o / L \ll 1$ and $(\omega_a - \omega)/\omega \ll 1$. Equation (1.2.1.) is used in (1.1.1) for T. M. modes and (1.2.3) is used in (1.1.1) for T. E. modes. The integration variable, dv, is written in the form, $r d\theta \, dr dz$. In this way it can be shown that for T. E. modes

$$\frac{2(\omega_a - \omega)}{\omega} = \frac{1^2 \left[\frac{n\pi}{L}\right]^2 \zeta_o \int_o^{2\pi} \sin^2(l\theta) \cos(s\theta) d\theta \int_o^{K(l,m)A} J_\ell^2 \frac{(x) J_s(\gamma x)}{x} dx}{N_B^2 K^2} \qquad (1.3.1)$$

$$+ \left[\frac{n\pi}{L}\right]^2 \frac{\zeta_o}{K^4 N_B^2} \int_o^{2\pi} \cos^2(l\theta) \cos(s\theta) d\theta \int_o^{K(l,m)A} \left[J_\ell'(x)\right]^2 J_s(\gamma x) \times dx$$

where $J_\ell' (x) = \frac{d}{dx} J_\ell (x)$

and

$$\gamma = \frac{K\,(S,\ P)}{K\,(1,\ m)}\ .$$

Similarly it can be shown that for T. M. modes

$$\frac{2(\omega_a - \omega)}{\omega} = \frac{\xi_o}{N_B^2}\int_0^{2\pi}\cos^2(1\theta)\cos(S\theta)\,d\theta\int_0^{K_o(l,m)A}\left[J_l'(x)\right]^2 J_S(\alpha x)\,x\,dx$$
$$+\frac{l^2\,\xi_o}{N_B^2}\int_0^{2\pi}\sin^2(l\theta)\cos(S\theta)\,d\theta\int_0^{K_o(l,m)A} J_l^{\,2}(x)\,\frac{Js\,(\alpha x)}{x}\,x\,dx$$
$$-\frac{\omega^2 K_o^{\,2}\,\xi_o}{k^4 N_E^2}\int_0^{2\pi}\cos^2(1\theta)\cos(S\theta)\,d\theta\int_0^{K_o(l,m)A} J_l^{\,2}(x)\,Js\,(\alpha x)\,x\,dx \qquad (1.\ 3.\ 2)$$

where

$$\alpha = \frac{K\,(S,\ P)}{K_o\,(1,\ m)}\ .$$

It is only necessary to compute one of the normalization constants, $N_B^{\,2}$ and $N_E^{\,2}$, because they are simply related. This can be shown by using Poynting's theorem (ref. 1). Poynting's theorem states that

$$\int_S(\hat{E}\times\hat{B})\cdot d\hat{s} + \frac{\partial}{\partial t}\int_V\left[\frac{\hat{B}\cdot\hat{B}}{2\mu} + \frac{\hat{E}\cdot\hat{E}\epsilon}{2}\right]dV = -\int_V \hat{E}\cdot\hat{J}\,dV\ .$$

S is the surface enclosing the volume V. $\hat{J}$ is the current density in V. Let V be the volume of the microwave cavity, V_c. As a result, $\hat{J} = 0$. Also, $\hat{E}\times\hat{B}\cdot d\hat{s} = 0$ because the electric field tangential to the surface S is zero. This is a consequence of the assumption that the conductivity of the cavity walls is very high (assumption iii above). Therefore,

$$\int_{V_c}\left[\frac{\hat{B}\cdot\hat{B}}{2\mu} + \frac{\hat{E}\cdot\hat{E}\epsilon}{2}\right]dv = \text{constant}\ .$$

Equations (1. 2. 1) and (1. 2. 3) show that $\hat{B}$ and $\hat{E}$ are out of phase by 90°. That is, when $\hat{E} = 0, \hat{B} = \hat{B}$ max. and when $\hat{B} = 0$, $\hat{E} = \hat{E}$ max. Therefore,

$$\int_{V_c}\left[\frac{\hat{B}\cdot\hat{B}}{2\mu} + \frac{\hat{E}\cdot\hat{E}\epsilon}{2}\right]dv = \int_{V_c}\frac{\hat{B}\ \text{max}\cdot\hat{B}\ \text{max}}{2\mu}\,dV = \int_{V_c}\frac{\hat{E}\ \text{max}\cdot\hat{E}\ \text{max}\,\epsilon}{2}\,dv\ .$$

But, $\hat{B}$ max $\cdot\ \hat{B}$ max $= |\hat{B}|^2$ and $\hat{E}$ max $\cdot\ \hat{E}$ max $= |\hat{E}|^2$.

As a result, $\int_{V_c}|\hat{B}|^2\,dv = \mu\epsilon\int_{V_c}|\hat{E}|^2 dV$ and so $N_B^{\,2} = \mu\epsilon\,N_E^{\,2}$.

It can easily be shown (by the use of equation 1. 2. 1) that for T. M. modes

$$N_B^2 = (1+\delta_{n0})\left\{(1+\delta_{\ell 0})\frac{\pi}{2}L K_0^2\int_0^A\left[J'(K_0 r)\right]^2 r\,dr + \ell^2\frac{\pi}{2}L\int_0^A \frac{J_\ell^2(K_0 r)}{r}dr\right\}$$

and

$$N_E^2 = N_B^2/(\epsilon\mu) \qquad \delta_{ij} = \begin{cases} 0 & i \neq j \\ 1 & i = j \end{cases} \qquad \text{(1. 3. 3)}$$

Similarly for T. E. modes it can be shown (by use of equation 1. 2. 3) that

$$N_B^2 = \epsilon\mu\, N_E^2$$

and

$$N_E^2 = \frac{\omega^2\pi L}{K^2 2}\left\{(1+\delta_{\ell 0})\int_0^A\left[J_\ell'(Kr)\right]^2 r\,dr + \frac{\ell^2}{K^2}\int_0^A \frac{J_\ell^2(Kr)}{r}dr\right\}. \qquad \text{(1. 3. 4)}$$

Equations (1. 3. 1) to (1. 3. 4) relate the change in resonant frequency of a cylindrical microwave cavity to the amplitude of a surface wave on a fluid acting as the end plate of that cavity.

The above calculations were made for a cylindrical cavity because this type of cavity was used during the experimental work. This type was used because it was easy to construct and to set up surface waves on a fluid within it. A rectangular cavity, however, has also been considered. Calculations similar to those above are given in appendix I. They show that a rectangular cavity acts as an automatic Fourier analyser. It appears that a rectangular cavity can be constructed so the change in resonant frequency of the cavity is directly proportional to only one Fourier component of the surface wave under investigation. The advantage of this feature is as follows. The theory of surface motion usually expresses the time and spatial dependence in terms of Fourier components. It is necessary, therefore, to Fourier analyse experimental data to obtain the time and spatial dependence of each Fourier component in order to make a comparison with theory. This tedious and complex analysing procedure may be eliminated by the automatic Fourier analysing feature of a rectangular cavity.

In the calculations for the rectangular and the cylindrical cavities it was found that the change in resonant frequency was proportional to the surface wave amplitude. This means that the observation of the surface wave's time dependence will be very easy. Also, an order of magnitude calculation using equation (1. 1. 1) shows that $\left(\frac{\omega_a - \omega}{\omega}\right) \simeq \frac{\xi_0}{L}$. Since values of 0.5×10^{-4} for $\left(\frac{\omega_a - \omega}{\omega}\right)$ are easily observed it means that the microwave system is sensitive to very small amplitude waves. These features, with the fact that the system is free of the problems associated with immersion devices, make the microwave system an extremely useful diagnostic tool for studying surface waves.

In order to use Slater's theorem to study surface waves it was considered necessary to test the important features of the theorem and to examine the conditions for which they are valid. This was done by introducing various, well defined shapes of known dimensions into the cavity at known positions. The work is reported in appendix 2. The results were found to be in agreement with the theory and it was concluded that Slater's theorem can be used to predict the change in resonant frequency of a microwave cavity caused by a small amplitude perturbation of the shape of that cavity.

The theoretical results of this chapter were used to develop a microwave system to study surface waves on mercury. The equipment and techniques used to study these waves are the topic of the next chapter.

Chapter 3 EXPERIMENTAL PROCEDURE, PARAMETERS, VARIABLES, AND ASSUMPTIONS

Section 1 EXPERIMENTAL PROCEDURE

The microwave system that was used is given in a block diagram in figure 2. Liquid mercury was placed in the bottom of the test cavity as shown in figure 3. The test cavity and microwave system were mounted on a large (1m.x1m.x1m) cement block to prevent any vibrations that might set up unwanted surface waves in the mercury. The test cavity was made of brass and nickel plated to prevent the mercury from reacting with the brass.

Three centimeter (8.6 to 9.6 KMc./s.) microwave equipment was chosen because it was easy to build the required test cavities and because of the availability and low cost of the components. The klystron (723 A/B) was the source of microwave power (a few milliwatts). Its output frequency was electronically modulated by a sawtooth voltage (from the oscilloscope) which was added to the repeller voltage of the klystron. In this way the output frequency of this klystron was changed by amounts up to 65 Mc./s. at modulation rates of up to 10,000 c./s. It was found that the change in output frequency of the klystron was directly proportional to the sawtooth voltage of the scope for changes up to 65 Mc./s. The isolator was used to prevent reflections caused by the wavemeter, magic tee, test cavity, etc. from changing the output power of the klystron. The calibrated wavemeter was used to determine the output frequency range of the klystron and to determine the resonant frequency of the microwave test cavities. The magic tee split the power from the klystron: one-half to the power terminator (which dissipated the energy) and one-half to the test cavity which dissipated or reflected the energy depending upon whether or not the output frequency of the klystron was equal to or not equal to the resonant frequency of the test cavity. The difference in power reflected from the power

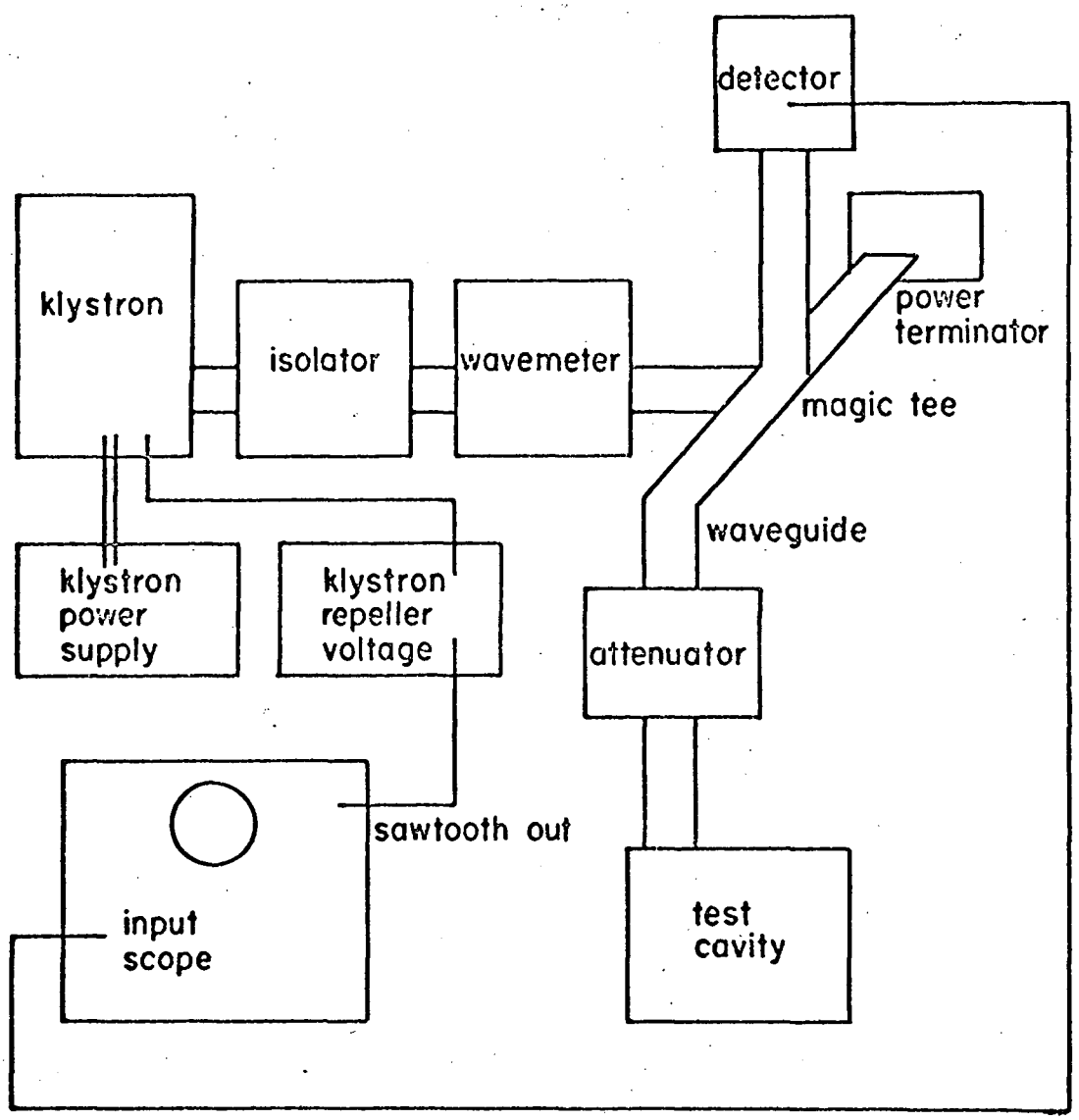

Fig. 2 Microwave system and test cavity.

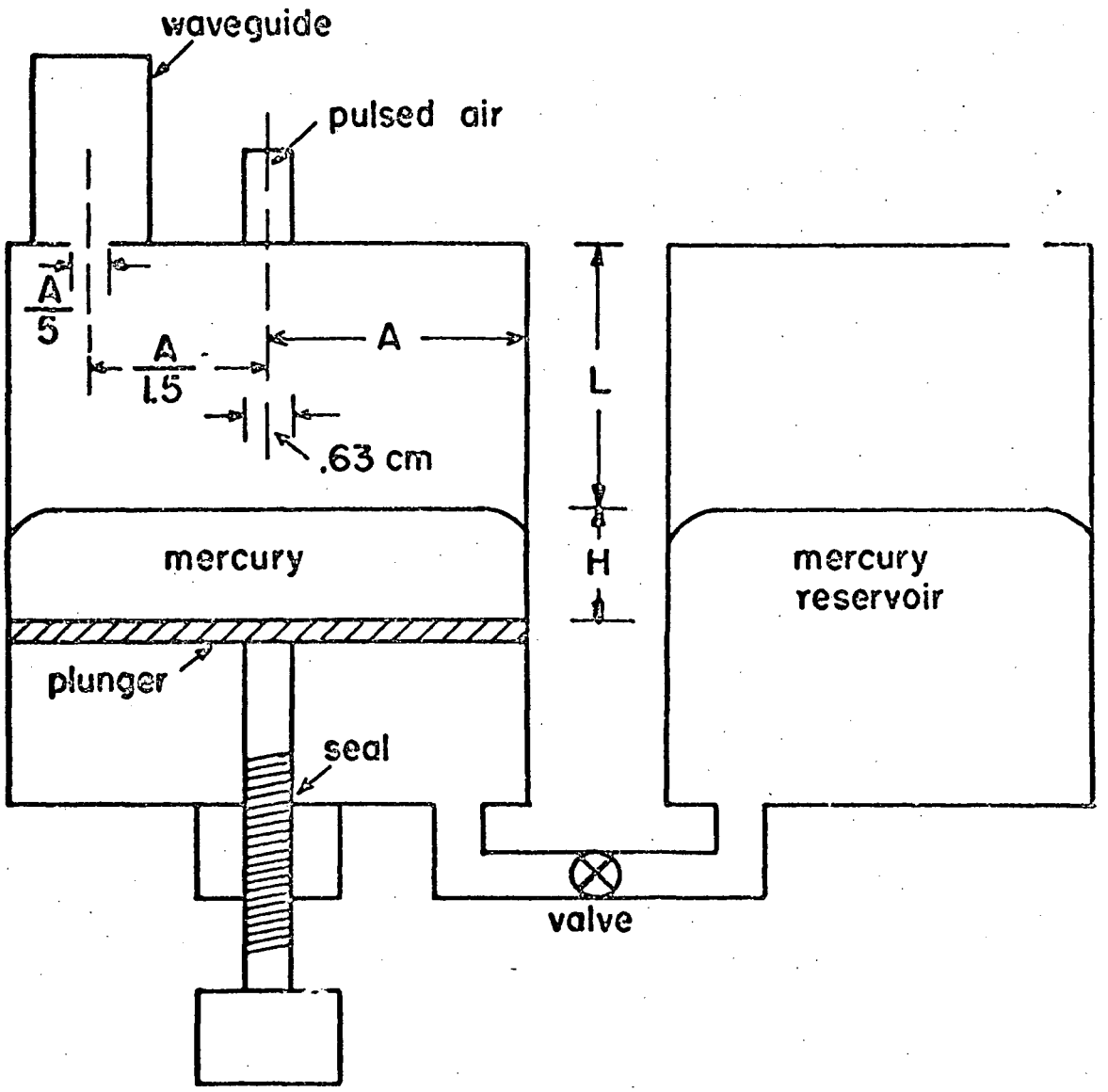

Fig. 3 Details of microwave test cavity.

terminator and the test cavity was detected by a crystal detector. The output voltage of the detector was a monotonic increasing function of the power detected and was applied to the vertical input of the scope. The nature of the resulting trace on the scope is shown in figure 4.

The Q_L of the system ($Q_L = \omega/$(banwidth of the resonant dip)) was found to be about 2000, as expected. An order of magnitude calculation (ref. 1) shows that

$$Q_L \simeq \frac{\text{Cavity volume}}{\left[\sum_i \sqrt{\frac{2}{\omega\mu g_i}}\, S_i\right]\left[1+\beta\right]}$$

where g_i is the electrical conductivity of the cavity wall surface, S_i, and β is the coupling coefficient. The coupling between the wave guide and cavity was varied until Q_L was a maximum. This corresponded to having $\beta \ll 1$. It was calculated from the above equation that the Q_L value could be increased by about 50% if copper or silver plating is used instead of nickel plating in the cavity. A Q_L of 2000, however, was more than adequate for measuring resonant frequency changes of .5Mc./s. or larger.

The depth of the mercury, H, was determined by the position of the plunger as shown in figure 3. The length of the cavity was varied (by varying the amount of mercury in the cavity) until an appropriate resonant em. mode was set up in the cavity (i.e. until a resonant "dip" was observed on the scope as in figure 4). This signal was expanded and the scope face masked off as shown in figure 5. The entire trace was masked off except for two small pieces which appeared as dots. The horizontal motion of these dots corresponded to the change in resonant frequency of the cavity. The horizontal motion of the peak of the resonant dip also corresponded to the change in resonant frequency of the cavity. The dots, however, were precisely defined whereas the peak of the resonant dip was not. Measurements

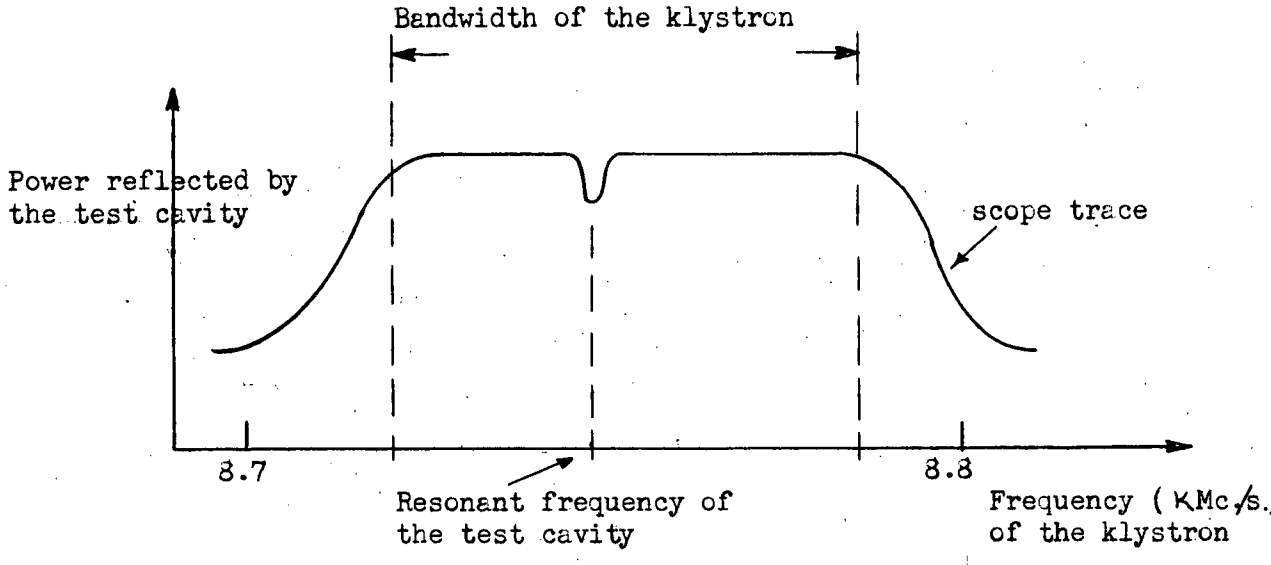

Figure 4. Details of the oscilloscope trace.

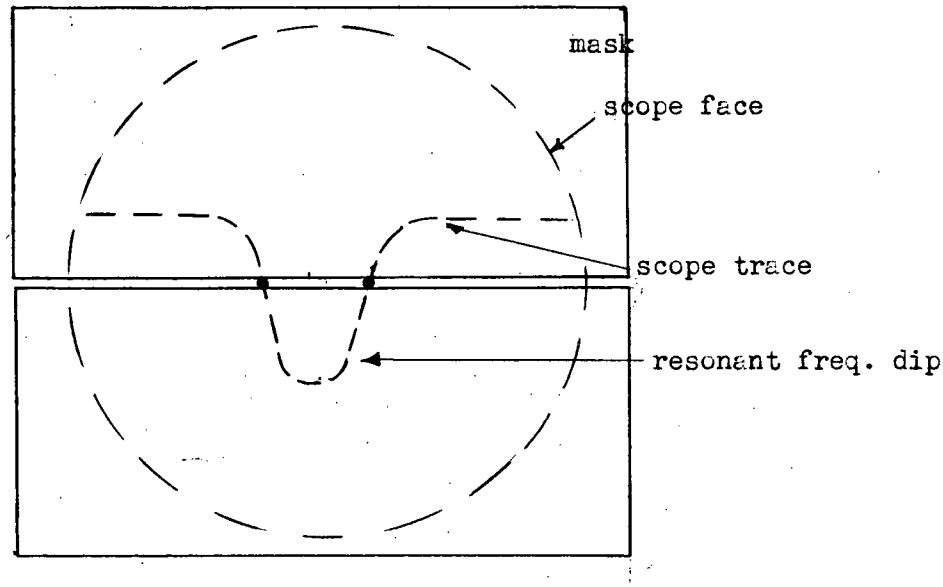

Figure 5 Method of monitoring the resonant frequency changes. The horizontal axis represents the kylstron frequency and the vertical axis represents the power reflected by the test cavity. The motion of the visible part of the scope trace was filmed.

were made to ensure that the horizontal motion of the dots (for resonant frequency changes of less than 2 Mc./s.) was due only to a change in resonant frequency and not due to a change in the shape of the resonant dip.

To set up axisymmetric, standing, surface waves on the mercury, air was pulsed into the cavity through a hole in the center of the cavity top (figure 3). Other workers such as Keuligan, Case and Parkinson (ref. 10 and 7) mechanically rocked the basin containing the fluid to set up surface waves. Fultz and Taylor, on the other hand, (ref. 11 and 12) used "flapgenerators." That is, they moved portions of the basin's walls to create surface waves. It was considered desirable to avoid these methods because the theories for surface waves assume that the basin is not in motion and that its walls are rigid. As a result, the method of setting up surface waves with pulsed air was developed.

The repetition rate of this pulsed air was varied (figure 6) until it was equal to the oscillation frequency of one of the "allowed" surface waves. At this point the "allowed" surface wave was set up. This caused the resonant frequency of the cavity to change. The air pulses were then turned off and the mercury wave was allowed to oscillate freely.

It has been shown (chapter 2, section 3) that the change in resonant frequency, $\omega_a - \omega$, is proportional to the amplitude of the surface wave, ζ_o. (Recall that $\zeta_o(t) = \zeta_o(0) \cos(2\pi f t) \exp(\sigma t)$.) Therefore, the time dependence of the horizontal motion of the two dots, seen on the scope face, is proportional to the time dependence of the surface wave in the cavity. This time dependence was continously recorded by continuously rolling film through a camera that was mounted on the scope face. In this way successive traces were photographed for an interval of about ten seconds.

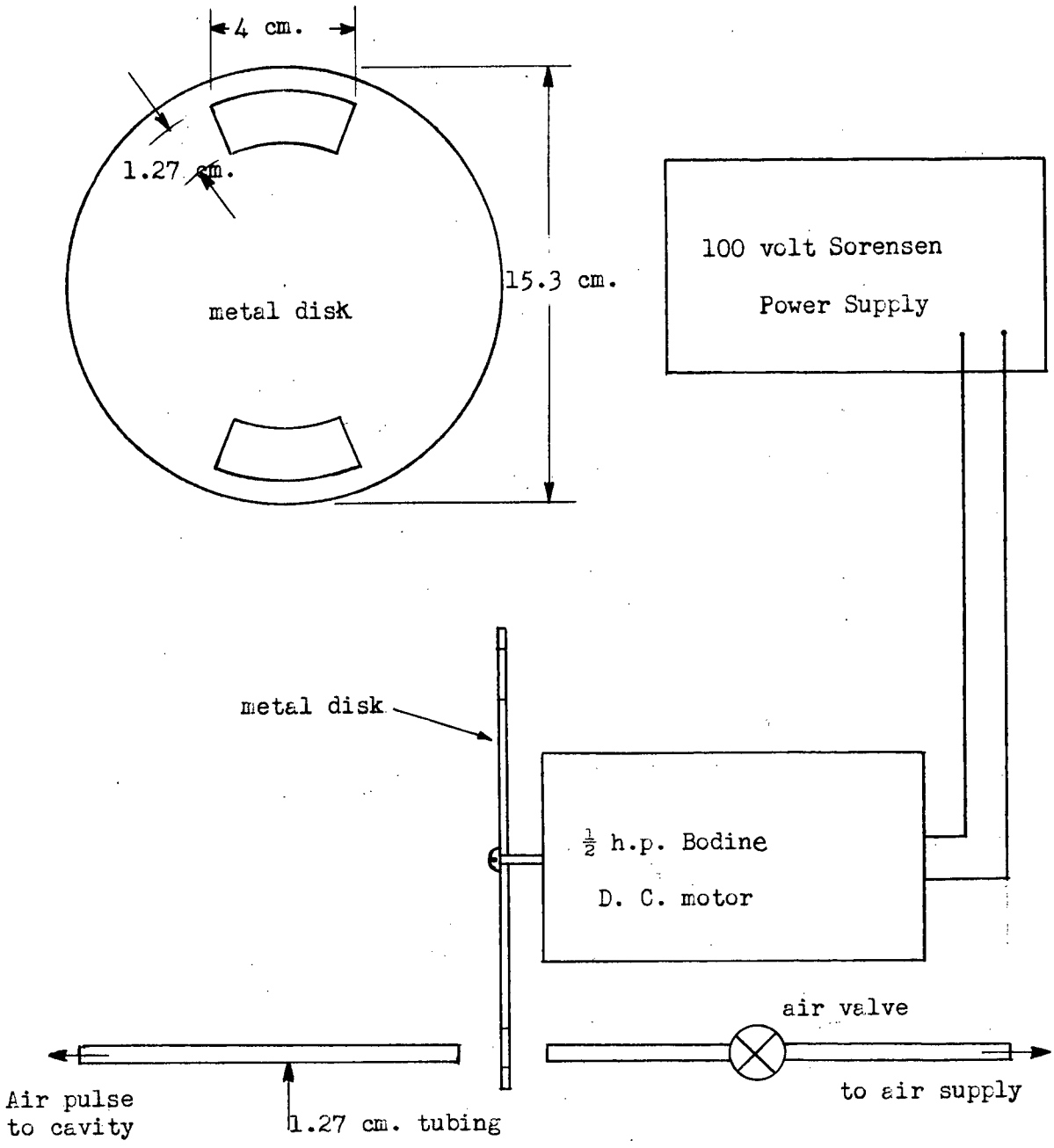

Figure 6. Method of producing air pulses to set up surface waves.

The nature of the resulting negative is seen in figure 7.

From similar negatives the values of $\zeta_0(0)$, f and σ were found for various conditions. The oscillation frequency, f, was found by counting the number of traces that occurred during ten complete oscillations of the surface wave. The trace time was measured by a time mark generator. The number of traces per ten oscillations could be measured to within $\frac{1}{2}\%$. Therefore, when the trace time was kept constant, oscillation frequency changes of $\frac{1}{2}\%$ or larger could be detected. The damping coefficient, σ, was measured by counting the number of oscillations of the surface wave that occurred as the amplitude decayed to e^{-1} of its original value and then using the oscillation frequency.

It was found that periodic surface waves were set up when the repetition rate of the air pulses was within 5% of f. Furthermore, no change in f (i.e. less than $\frac{1}{2}\%$ change in f) was found when the repetition rate was varied within 5% of f. This indicates that the oscillation frequency, f, of the particular surface wave that was created was independent of the method used to create the wave.

During a number of experiments the effect of a uniform, constant, vertical, applied magnetic field was studied by placing the test cavity and fluid in the magnetic field at the center of a solenoid (figure 8). The solenoid consisted of 5 coils of #11 copper wire in parallel. Each coil consisted of 150 turns. Twenty-four volts across the solenoid caused an input current of about 600 amperes. This resulted in a magnetic field of about 2200 gauss at the center of the solenoid. This field was independent of position (i.e. varied by less than 3%) in the volume indicated in figure 8. The mercury was placed in this volume when the effect of a magnetic field on a surface wave was studied. Switching the magnetic field on or off caused unwanted surface waves. These waves were allowed to damp out before

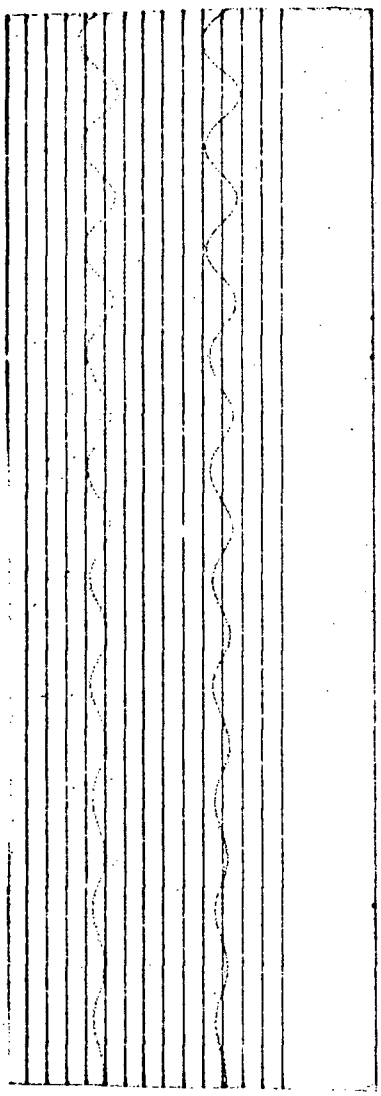

Figure 7. A record of the time dependence of a surface wave amplitude. The above is a 120 film negative taken of the horizontal motion of the scope trace shown in figure 5. The horizontal position of each dot represents the change in the resonant frequency of the test cavity which is proportional to the amplitude of the surface wave in the cavity. The vertical axis represents time.

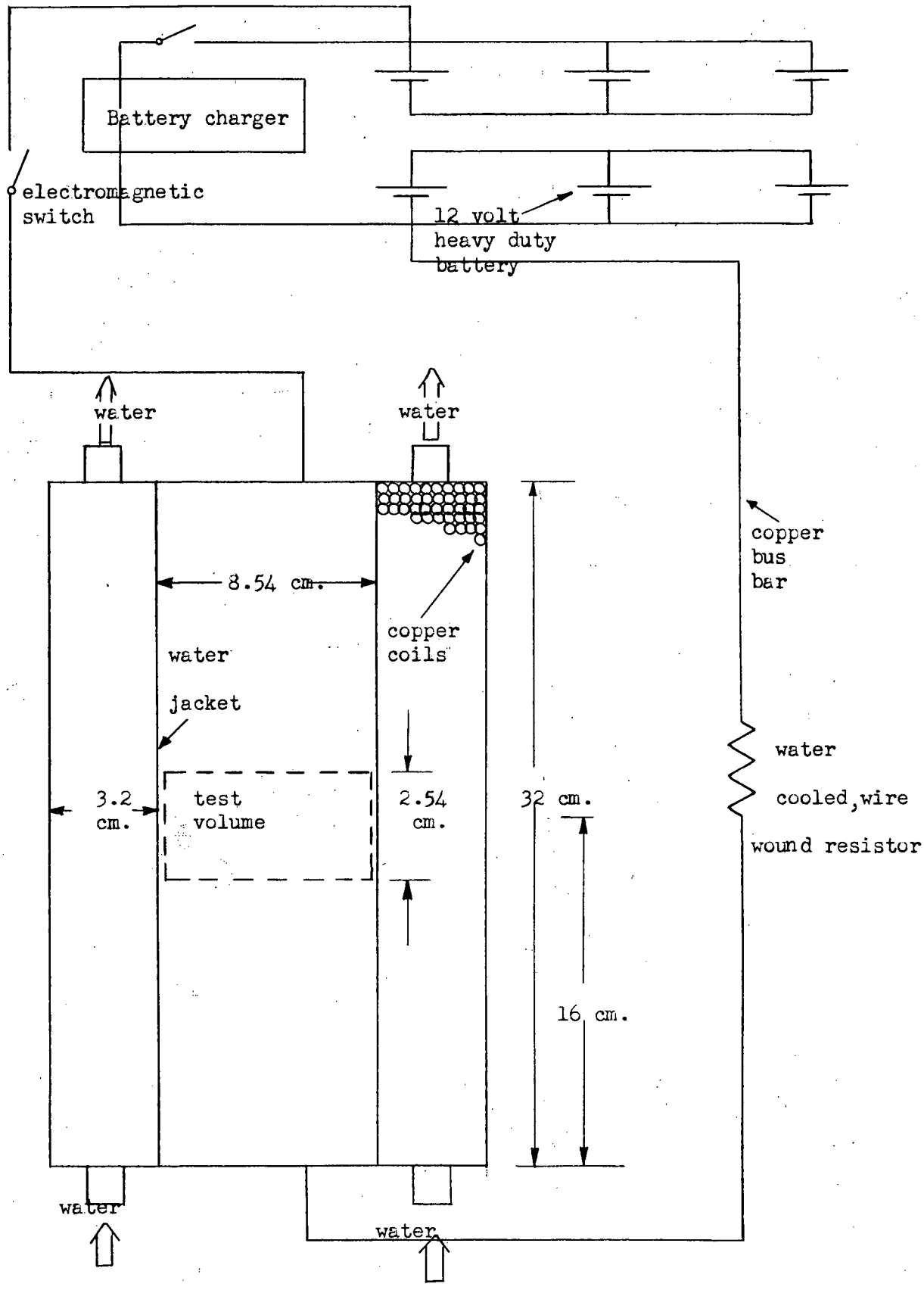

Figure 8 Method of producing a uniform, constant, magnetic field.

a controlled wave was set up and investigated. The strength of the magnetic field was measured by a Bell 240 incremental gaussmeter.

Section 2 PARAMETERS, VARIABLES, AND ASSUMPTIONS

The oscillation frequency and the damping coefficient of a surface wave have been measured for a variety of parameters.

During all experiments described in this chapter and in the following chapters this surface wave was of the form $\zeta = \zeta_o(t)\ J_s(K(S,P)\,r)\cos(S\theta)$. The standard theory of fluid surface waves (ref. 6 or equation (4. 1. 1)) was used to compute K (S, P) from the measurement of the oscillation frequency. The valves of S and P were then found by consulting the tables for K (S, P) A (ref. 5). Recall that $J_s'(K(S,P)A) = 0$ where A is the cavity radius. The study was restricted to waves where $S = 0$ and $P = 2$. By keeping S and P constant the "shape" or "type" of wave was kept constant. From the tables of reference 5 it was found that $K(0,2)A = 1.2197\pi$. Three different values of K were used by using three different cavity radii ($A = 2.54$, 3.17 and 3.64 cm.).

In all surface wave experiments the em. mode in the resonating cavity was either the TE_{211} or the TE_{111} mode. A computer program was used to calculate $\left(\frac{\omega_a - \omega}{\omega \zeta_o}\right) L$ from equations (1. 3. 1) and (1. 3. 2). This calculation was only used to measure the magnitude of ζ_o. This was done to ensure that the linear or small amplitude assumptions were valid for the waves under investigation. The study of the damping coefficients and the oscillation frequencies, however, relied only upon the fact that $\omega_a - \omega$ is proportional to ζ_o

Table 1 summarises the parameters and variables for which the oscillation frequencies and damping coefficients were measured.

In order to isolate the magnetic damping coefficient, σ_B , from the observed, total damping, σ , ($\sigma = \sigma_o + \sigma_B$) the viscous damping coefficient, σ_o, and also the oscillation frequency have to be measured. The following two chapters describe this work.

SUMMARY OF DEFINITIONS AND CONSTANTS USED IN TABLE 1

A	=	cavity radius
K	=	radial wave number of surface waves
S	=	0 P = 2 KA = 1.2197 π
T	=	surface tension of mercury = 490 dynes/cm.
ρ	=	mass density of mercury = 13.6 g./cm.
ν	=	kinematic viscosity of mercury
	=	Q11 centipoises cm.^{3}/g.
g	=	gravitational constant = 980 dynes/g.
σ	=	electrical conductivity of mercury
	=	1.04 x 10^6 (ohm meter)$^{-1}$
H	=	depth of mercury
σ_f	=	damping coefficient of the surface wave
ξ_o	=	oscillation frequency of the surface wave
B_3	=	surface wave amplitude
L	=	applied vertical magnetic field
n	=	length of the microwave cavity
$\omega_a - \omega$	=	axial mode number of em. mode in the cavity
ω	=	change in resonant frequency of the cavity
R_m	=	resonant frequency of the microwave cavity
		magnetic Reynolds number

Table I Parameters, Variables and Assumptions used during surface wave experiments

Variables and Parameters	Assumptions used in theory	Experimental values		
Cavity number		I	II	III
A (cm)		2.54	3.17	3.64
K (cm.$^{-1}$)		1.51	1.21	1.05
em. mode used		TE_{211}	TE_{111}	TE_{111}
δ_o range (cm.)		.04 - .01	.0015 - .0007	.0015-.0007
H range (cm.)		0.4 - 4.0	0.4 - 4.0	0.4-4.0
B_3 (gauss)		0 - 2200	0 - 2200	0-2200
f (c/s.)		4.6 - 7.0	3.5 - 5.8	3.5-5.2
$n\pi\delta_o/L$	$\ll 1.0$	$\leqslant 0.1$	$\leqslant 0.004$	$\leqslant 0.004$
$(\omega_a - \omega)/\omega$	$\ll 1.0$	$\leqslant .002$	$\leqslant .002$	$\leqslant .002$
δ_o / H	$\ll 1.0$	$\leqslant .06$	$\leqslant .0005$	$\leqslant .0005$
$\delta_o K$	$\ll 1.0$	$\leqslant .03$	$\leqslant .002$	$\leqslant .002$
$\delta_o K/(KH)^3$	$\ll 1.0$	$\leqslant .5$	$\leqslant .04$	$\leqslant .04$
$\left[\frac{\nu}{2\pi f}\right]^{\frac{1}{2}}/\left(\frac{2\pi}{K}\right)$	$\ll 1.0$	$\leqslant .0006$	$\leqslant .0006$	$\leqslant .0006$
$\left[\frac{\nu}{2\pi f}\right]^{\frac{1}{2}}/(H)$	$\ll 1.0$	$\leqslant .015$	$\leqslant .015$	$\leqslant .015$
$\left[\frac{\nu}{2\pi f}\right]^{\frac{1}{2}}/(A)$	$\ll 1.0$	$\leqslant .001$	$\leqslant .001$	$\leqslant .001$
$\sigma_o/(2\pi f)$	$\ll 1.0$	$\leqslant .02$	$\leqslant .02$	$\leqslant .02$
ρ = CONSTANT		mercury used		
$g B_3^2/(\rho 2\pi f)$	$\ll 1.0$	$\leqslant .2$	$\leqslant .2$	$\leqslant .2$
$\mu g v l \equiv R_m$	$\ll 1.0$	$\leqslant .01$	$\leqslant .01$	$\leqslant .01$

Chapter 4. STUDY OF THE OSCILLATION FREQUENCY OF A SURFACE WAVE IN MERCURY

The microwave cavity technique was used to investigate the relation between the oscillation frequency, f, the fluid depth, H, and the radial wave number, K, of a linear, standing, gravity surface wave. The oscillation frequencies were studied for both deep and shallow fluid waves. KH was varied from about 0.4 to about 3.0. Figure 10 is typical of the time dependence of the waves that were studied. It shows that the time dependence was sinusoidal, as expected. The oscillation frequencies were measured and summarised in figures 9A and 9B.

The linearized theory of standing surface waves on an ideal, incompressible fluid (ref. 6) shows that $(2\pi f)^2 = \left(\frac{TK^3}{\rho} + gK\right) \tanh(KH)$. (4.1.1)

Table 1 contains the relevant definitions and a list of the assumptions which were made in order to develop the above equation. Equation (4. 1. 1) was plotted using the valves for T, ρ, and KA given in table 1 for various A's. These plots (fig. 9a) indicate that the oscillation frequency depends on the basin radius, A, and the fluid depth, H, as predicted by the theory. It was noted, however, that the observed frequencies were larger than the theoretical ones by 10 to 15%.

Discrepancies of this nature have been noted by other workers (ref. 7). The difference between experiment and theory may be due to:

(1) experimental error in measuring f,

(2) the assumptions of the linear theory not being valid,

(3) an error in the value of T/ρ that was used,

(4) surface tension effects associated with the meniscus.

Each of these possibilities will now be considered.

(1) The maximum percent error in measuring f was less than 2%. Therefore, the differences between the experiment and the theory (approx. 10%)

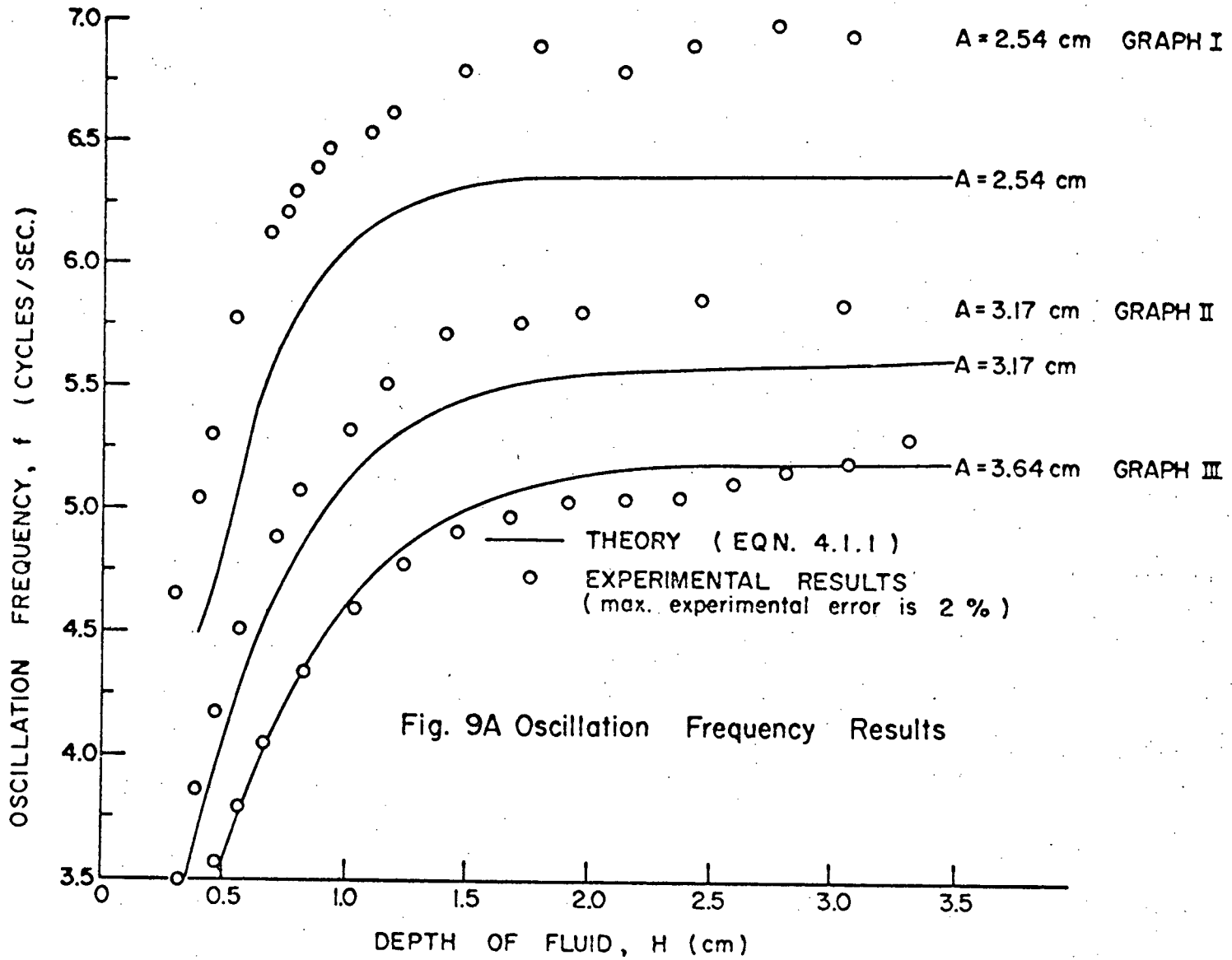

Fig. 9A Oscillation Frequency Results

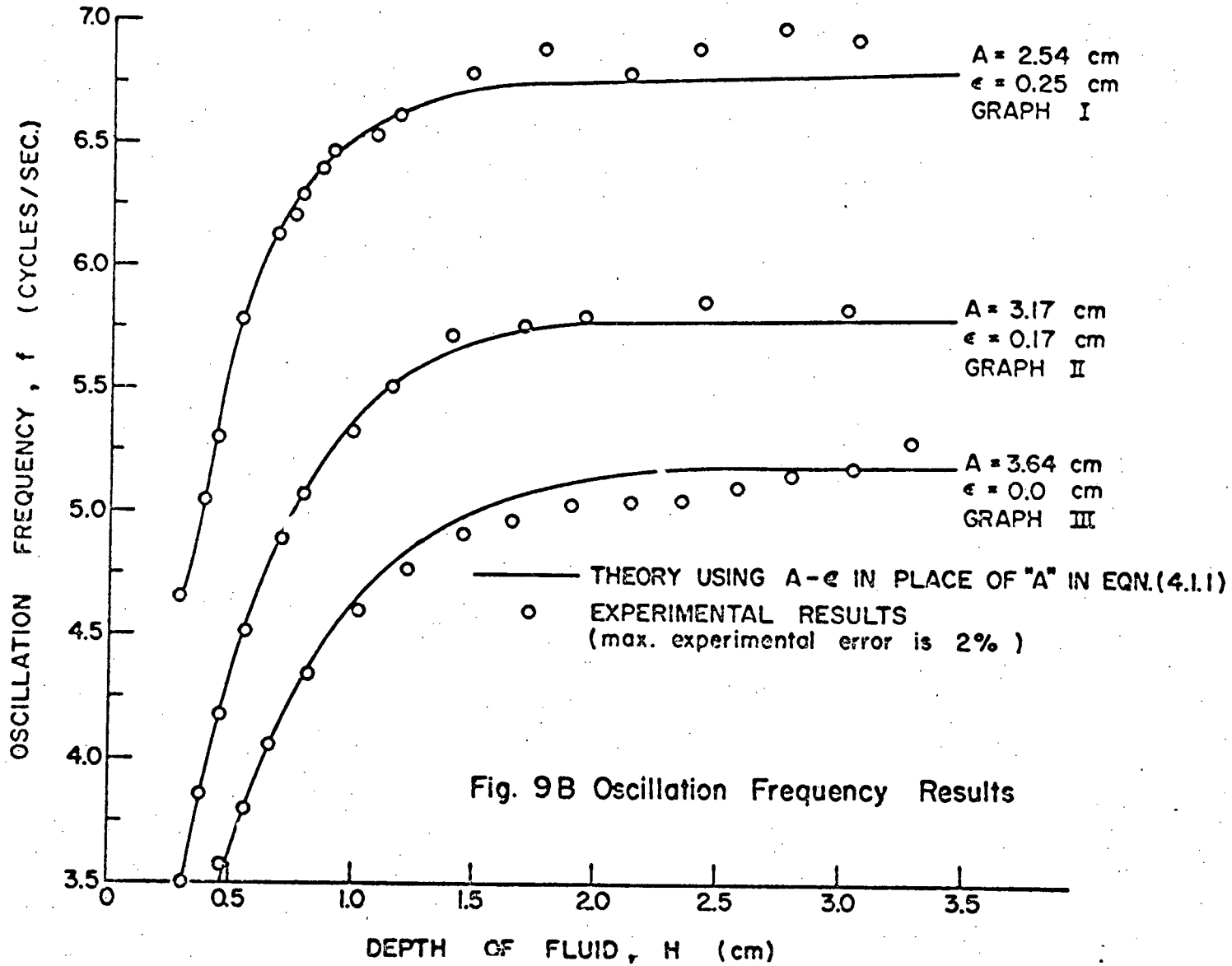

Fig. 9B Oscillation Frequency Results

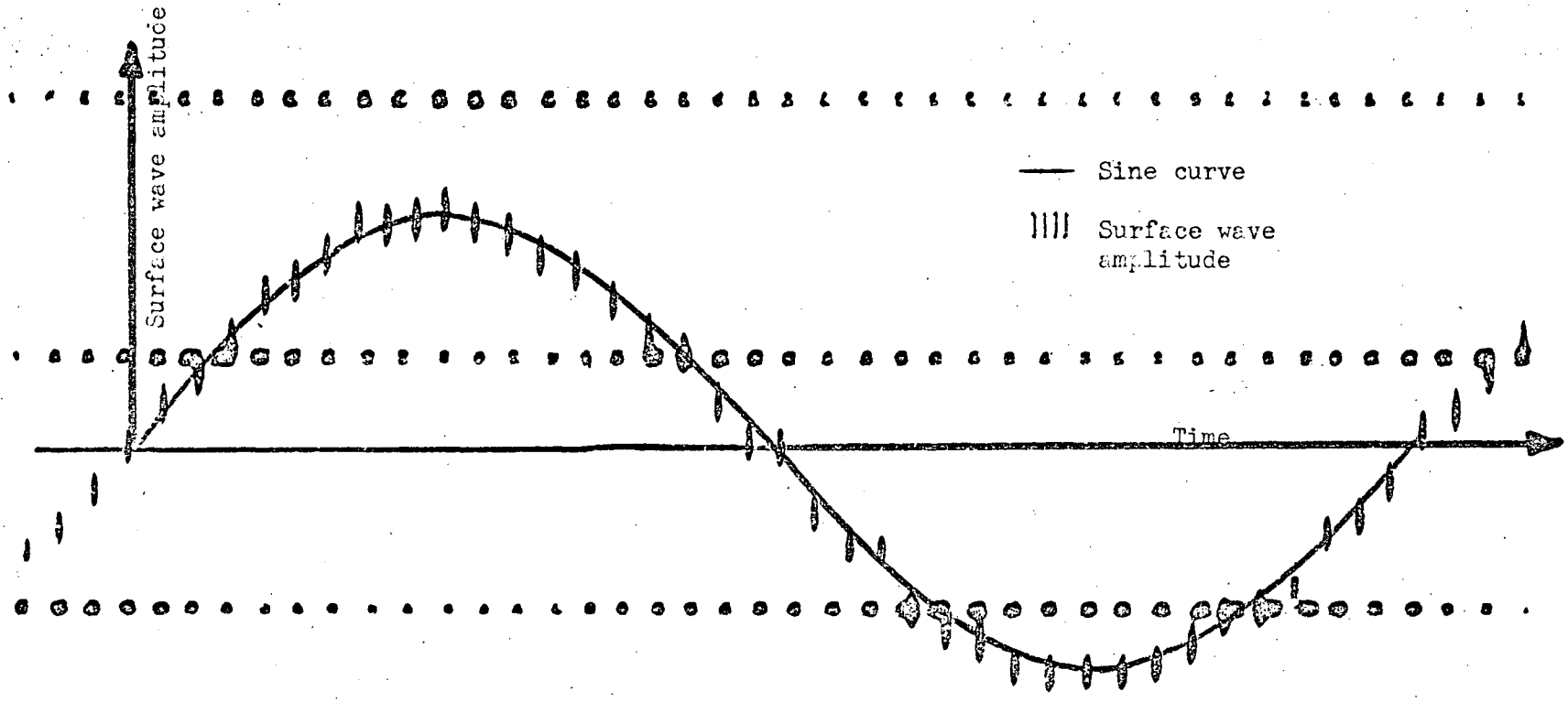

Figure 10. Sinuscidal time dependence of a typical surface wave.

cannot be explained in this way.

(2) Table 1 shows that all of the assumptions of the theory were satisfied during the experiment.

(3) It is well known that contamination of a surface can decrease the surface tension, T. (ref. 9). However, $\frac{TK^3}{\rho} < 10\%$ of g K for our experiments. Therefore, T would have to be increased by 200% to account for the difference between experiment and theory. (See equation (4.1.1).)

(4) The equation for f results from evaluating a linearized form of the equation of motion of the fluid at the surface. The value of K is determined by using the boundary condition, $V_r = 0$ at $r = A$ (V_r is the radial velocity of the fluid). It is conceivable, however, that because of the meniscus this boundary condition is not true at the surface. It is suggested that the condition $V_r = 0$ at $r = A - \epsilon$ (where ϵ is defined in figure 11) is more realistic at the surface. This would result in K and, therefore, f being evaluated by $A - \epsilon$ instead of A.

During the experiments corresponding to graphs I and II of figure 9 ϵ was measured and found to be of the order of 0.2 cm. Figure 9b shows that the use of ϵ values of this size to calculate f for these two experiments results in agreement between theory and experiment. During the experiment of graph III, figure 9b, ϵ was less than .02 cm. This low value was presumably due to surface contamination during this experiment. Figure 9b shows that the use of an ϵ value of this size to calculate f for this experiment again results in agreement between theory and experiment.

Another experiment to test the dependence of f on ϵ was performed for H $\pm$ 1.00 cm. and A $\pm$ 3.64 cm. The results showed that ϵ was of the order of 0.2 cm. when fresh, clean mercury was used. The oscillation frequency agreed with the theory when A - 0.25 cm. was used instead of A.

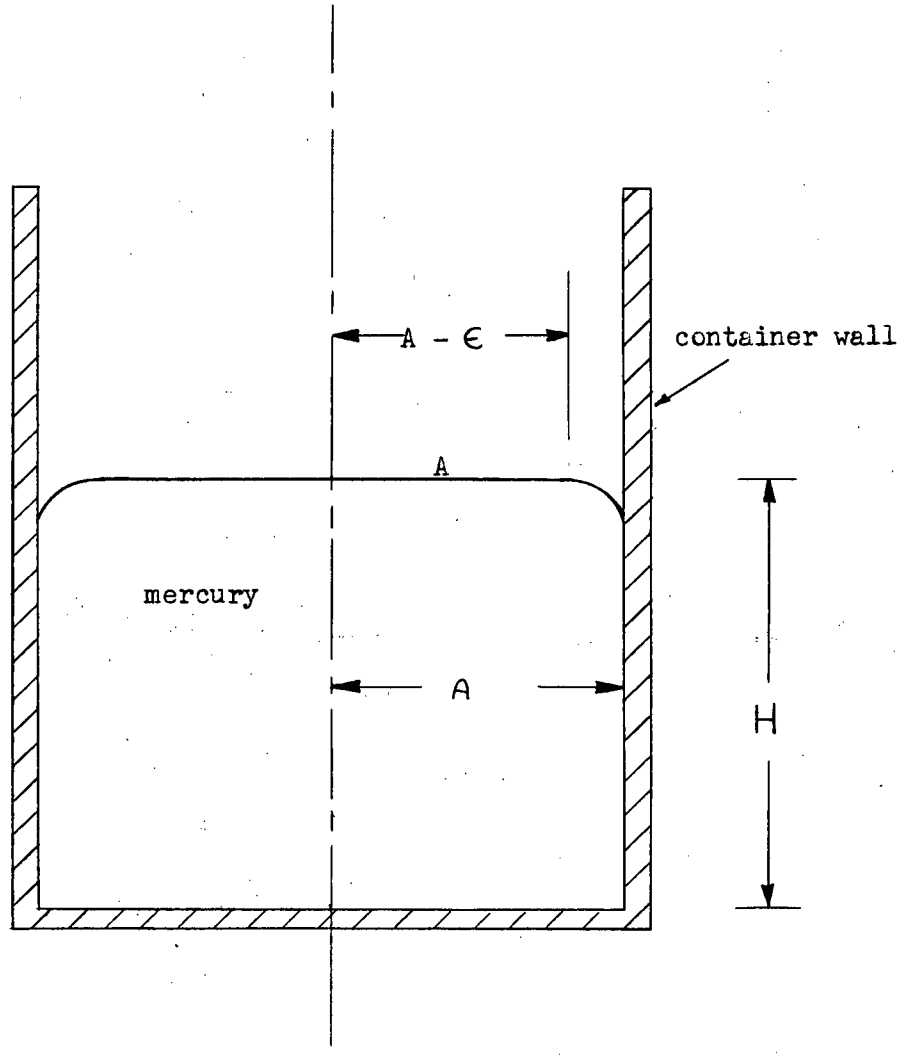

Figure 11 Surface distortion due to surface tension.

After a film of oil, dust and mercury oxide was introduced the value of ϵ was found to be of the order of 0.02 cm. The oscillation frequency was then found to agree with the theory using A - 0.02 cm.

These results suggest that the meniscus is responsible for the 10% discrepancy between the theoretical and experimental values for the oscillation frequency.

CHAPTER 5

STUDY OF THE VISCOUS DAMPING OF A SURFACE WAVE IN MERCURY

The time dependence of a small amplitude, standing wave is given by $\exp(\sigma_o t)\sin(2\pi f t)$. The microwave cavity technique was used to investigate the relation between the viscous damping coefficient, σ_o, the fluid depth, H, and the radial wave number, K, of a linear, standing, gravity, surface wave.

The viscous damping of surface waves was studied for both deep and shallow fluid waves. KH was varied from about 0.4 to about 3.0. Figure 12 shows how the surface wave amplitude decayed. It shows that the waves decayed exponentially, as expected. The damping coefficient was measured and the results summarised in figure 13.

The standard, linearized theory of axisymmetric, standing waves in an incompressible fluid is given by Case and Parkinson (ref. 7). They show that

$$\sigma_o = \sigma_v + \sigma_w + \sigma_b + \sigma_s \qquad (5.1.1)$$

σ_v is the damping coefficient due to the energy dissipation in the body of the liquid. σ_w is due to the boundary layer at the side walls. σ_b is due to the boundary layer at the bottom wall of the fluid container and σ_s is due to the dissipation in the boundary layer at the free surface of the fluid. They find the following:

$$\left.\begin{aligned}
\sigma_v &= -2\nu K^2 \\
\sigma_w &= -\sqrt{\frac{\nu 2\pi f}{2}}\,\frac{K}{(AK)2}\left(\frac{1+(S/KA)^2}{1-(S/KA)^2} - \frac{2KH}{\sinh(2KH)}\right) \\
\sigma_b &= -\sqrt{\frac{\nu 2\pi f}{2}}\,K\left(\frac{1}{(\sinh(2KH))}\right) \\
\sigma_s &= 0
\end{aligned}\right\} \qquad (5.1.2)$$

where $(2\pi f)^2 = \left(\frac{TK^3}{\rho} + gK\right)\tanh(KH)$ and ν is the kinematic viscosity of the fluid. The assumptions that were used to develope this theory are given in table 1.

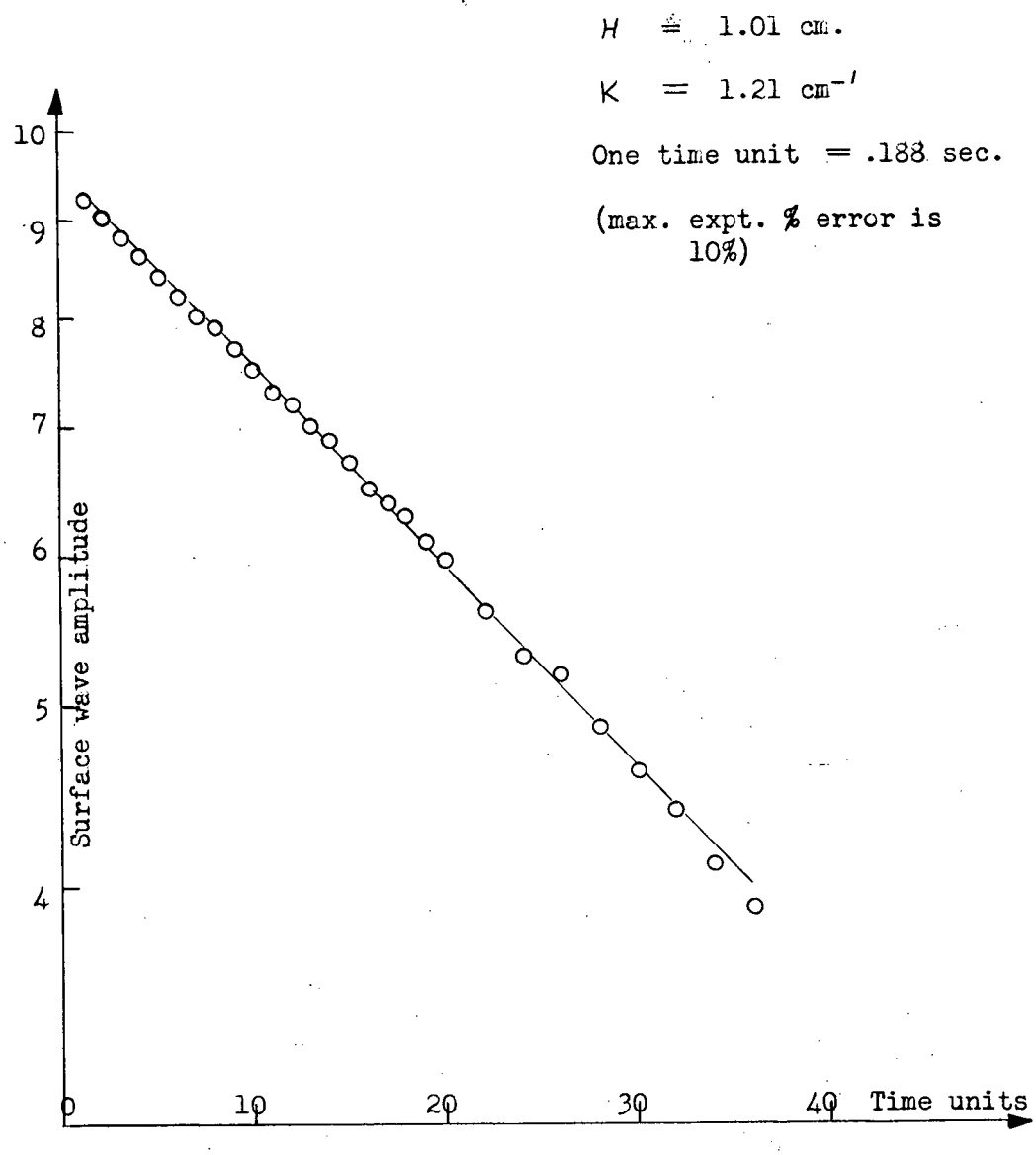

Fig. 12 graph showing the exponential decay of a typical surface wave.

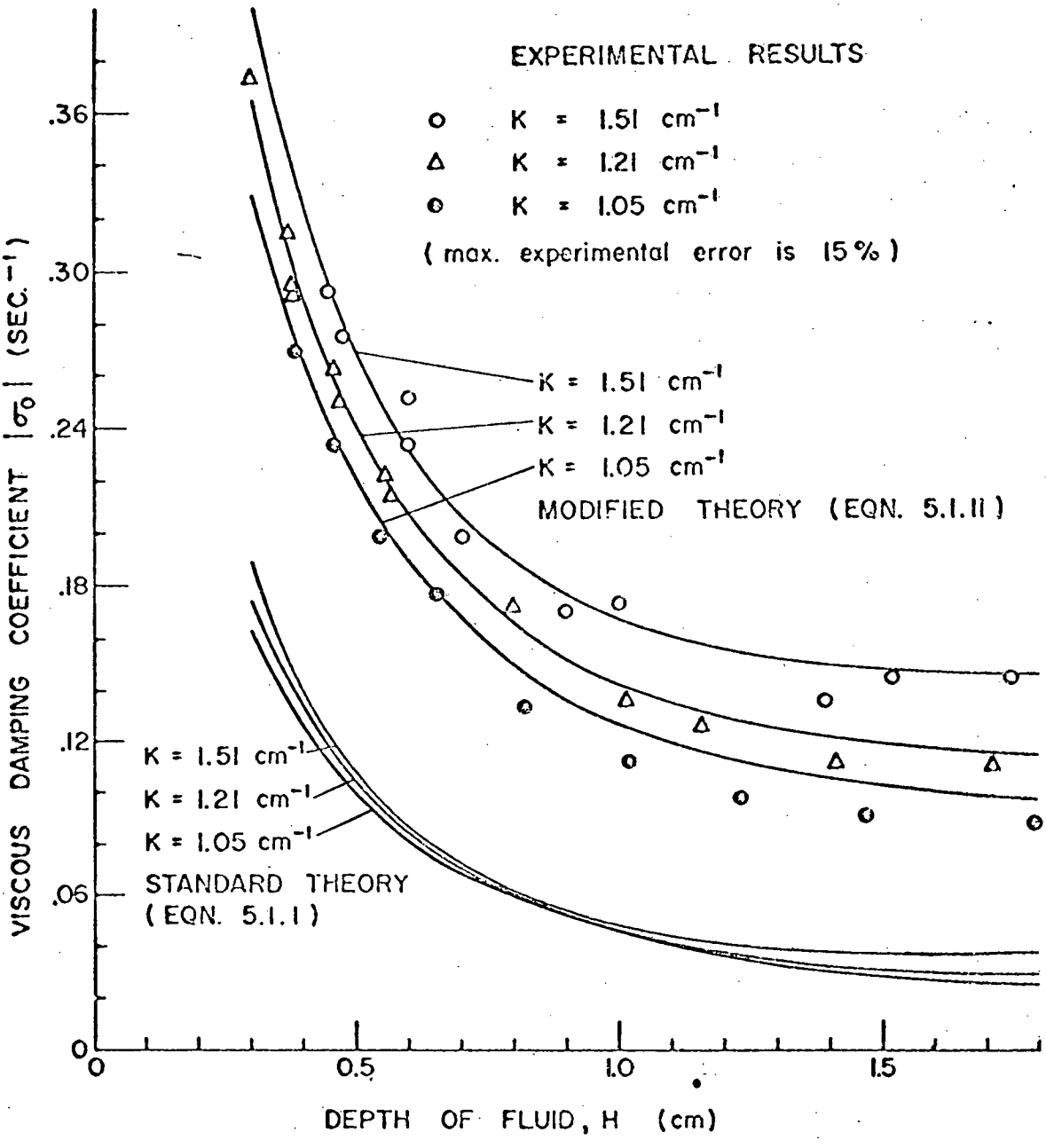

Fig. 13 Viscous Damping Coefficient Results

The boundary conditions were the following:

(i) The fluid velocity is zero at the rigid boundaries.

(ii) The flow is irrotational at the free surface.

The above equation for $|\sigma_o|$, (5. 1. 1) and (5. 1. 2), was plotted in figure 13 using the experimental values given in section 2, chapter 3. Figure 13 indicates that the experimental values of σ_o were larger than predicted by Case and Parkinson's theory by up to a factor of 4. Discrepancies of this nature have been noted and, in some cases, accounted for by people working on other surface wave experiments (ref. 10, 14, 16, 17, 18). The difference between experiment and theory may be due to

(1) systematic errors (i.e. experimental error in measuring σ_o),

(2) a damping effect due to em. fields in the microwave cavity,

(3) violations of the linearity assumptions used to develop the theory,

(4) rough boundaries,

or (5) the use of an invalid boundary condition.

Each of these possibilities will now be considered.

(1) The systematic percent error (i.e. the percent error in the measurement of σ_o) could be as high as 15%. The graph of figure 13 shows that there was a difference between experiment and theory of up to about 400%. The systematic error, therefore, could not account for it.

(2) An experiment was performed to investigate the effect of the microwave cavity's em. field on the damping of the surface waves. An attenuator was used to vary (by a factor of 3) the power absorbed by the cavity during resonance. In this way σ_o was measured for various values of the cavity's em. field. Results showed that σ_o varied by less than 5%. It was concluded, therefore, that σ_o was independent of the cavity's em. field.

(3) Other workers have not always satisfied all the linearizing assumptions given in table 1. The assumption $\zeta_0 K \ll (HK)^3$ is, in some cases, not even included in the theoretical discussions (ref. 7, 10, 17). Hunt and Ursell (ref. 18 and 13) have pointed out this omission. In many cases (ref. 7, 14 and 17) workers have violated this assumption during their experiments in shallow water (i.e. $KH \simeq 0.1$). This happened because they had difficulty observing surface waves such that $\zeta_0 K \ll (0.1)^3$. Table 1, however, shows that all of the assumptions (including $\zeta_0 K \ll (KH)^3$) were satisfied in our experiments. The high sensitivity of the microwave system made this possible.

(4) Case and Parkinson (ref. 7) noticed an effect which was apparently due to wall roughness. They found that the experimental damping coefficient was two to three times larger than their theory predicted until they highly polished the container walls. Even a roughness of depth less than the boundary layer thickness appeared to increase the rate of damping. After polishing the container they found that their experimental results agreed to within 15% of their theory. Other experimenters (ref. 19 and 20), however, found that σ_0 was independent of wall roughness. In view of this and in view of later work on surface wave damping due to surface films, it is suggested that the Case and Parkinson discrepancy was, in fact, due to a film on the water surface. For our experiments the cavities were plated with a hard nickel and then highly polished.

(5) The theory of Case and Parkinson (equations (5. 1. 1) and (5. 1. 2)) assumes that the fluid motion is irrotational at the fluid surface. If, however, this assumption is replaced by the assumption that there is no horizontal, fluid velocity at the surface then the theory will be altered. The following is an outline of how the Case and Parkinson theory was

modified by the author using this new boundary condition in an attempt to explain the experimental results of figure 13.

Case and Parkinson used standard, boundary layer theory and let $\hat{V}$, the fluid velocity, equal $-\hat{\nabla}\phi + \hat{\nabla} \times \hat{A}$. $\hat{\nabla}\phi$ is the fluid velocity that would exist if $\nu = 0$ and $\hat{\nabla} \times \hat{A}$ is the correction that must be added to $\hat{\nabla}\phi$ to satisfy the additional boundary condition that occurs when $\nu \neq 0$. When $\nu \neq 0$ the fluid velocity tangential to a wall is zero. Case and Parkinson show that

$$\phi = C_1 \cosh(Kz) \cos(s\theta)\, Js(Kr) \cos(2\pi f t) \exp(\sigma_o t) \qquad (5.1.3)$$

where C_1 is a constant.

The approximations used in boundary layer theory allow one to calculate σ_o from $\sigma_o = \sigma_v + \sigma_w + \sigma_b + \sigma_s$ (ref. 21) where

$$\left.\begin{aligned} \sigma_b &= C_2 \int_{V_b} (\hat{\nabla} \times \hat{\nabla} \times \hat{A})\, dV \\ \sigma_w &= C_2 \int_{V_w} (\hat{\nabla} \times \hat{\nabla} \times \hat{A})\, dV \\ \sigma_s &= C_2 \int_{V_s} (\hat{\nabla} \times \hat{\nabla} \times \hat{A})\, dV. \end{aligned}\right\} \qquad (5.1.4)$$

C_2 is an unimportant constant. V_b, V_w, V_s are volumes in the vicinity of the bottom wall, the side walls and the surface respectively. It is convenient to define $\hat{A}s$, $\hat{A}b$ and $\hat{A}w$ by

$$\left.\begin{aligned} \hat{A} &= \hat{A}s \text{ in volume } V_s \\ \hat{A} &= \hat{A}b \text{ in volume } V_b \\ \hat{A} &= \hat{A}w \text{ in volume } V_w \end{aligned}\right\} \qquad (5.1.5)$$

Case and Parkinson solved for $\hat{A}_b$ and $\hat{A}w$ by using the boundary condition resulting from the fact that $\nu \neq 0$. That is, they solved for $\hat{A}_b$ and $\hat{A}w$ from

$$\hat{I}_z \times (\hat{\nabla} \times \hat{A}_b) = \hat{I}_z \times \hat{\nabla}\phi \quad (z = 0) \qquad (5.1.6)$$

and

$$\hat{I}_z \times (\hat{\nabla} \times \hat{A}w) = \hat{I}_z \times \hat{\nabla}\phi \quad (r = A) \qquad (5.1.7)$$

using equation (5.1.3). They then solved for σ_b and σ_w by using equations (5.1.5) and (5.1.4).

They assumed that the flow was irrotational at the surface (i.e. $\hat{V} = -\hat{\nabla}\phi$). This meant that $\hat{A}s = 0$ and, therefore, $\sigma_s = 0$.

If, however, it is assumed that there is no horizontal fluid velocity at the surface then σ_s will not be zero because $\hat{A}s$ will not be zero. This is because "$\hat{V} = -\hat{\nabla}\phi$ at surface" is replaced by

$$\hat{I}_z \times \hat{V}\,(z = H) = 0 = -\hat{I}_z \times \hat{\nabla}\phi(z = H) + \hat{I}_z \times \hat{\nabla} \times \hat{A}s \quad (5.1.8)$$

All that remains is to use equation (5.1.3) in (5.1.8) to solve for $\hat{A}_s$ and then use (5.1.5) in (5.1.4) to solve for σ_s. This can be easily accomplished by noting in equation (5.1.3) that

$$\phi(z = H) = \phi(z = 0)\cosh(KH). \quad (5.1.9)$$

Using equation (5.1.9) in (5.1.8) and (5.1.6) it is obvious that $\hat{A}s = \hat{A}_b \cosh(KH)$. Using this with equations (5.1.4) and (5.1.5) gives $\sigma_s = \sigma_b \cosh^2(KH)$. From equation (5.1.2) we find, therefore, that

$$\sigma_s = -\sqrt{\frac{\nu 2\pi f}{2}}\, K\, \frac{\cosh^2(KH)}{\sinh(2KH)}. \quad (5.1.10)$$

It is reassuring to note that

$\sigma_s = -\sqrt{\frac{\nu 2\pi f}{2}}\, \frac{K}{2}$ for $KH \gg 1$ and that this agrees with the calculations made by Lamb and Levich (ref. 21 and 22). The total damping coefficient is found by using (5.1.10) in (5.1.1) and (5.1.2). It is

$$\sigma_o = -2\nu K^2 - \sqrt{\frac{\nu 2\pi f}{2}}\, K\left\{ \frac{1}{2A}\left[\frac{1 + (S/KA)^2}{1 - (S/KA)^2} - \frac{2KH}{\sinh(2KH)} \right] + \frac{1}{\sinh(2KH)} + \frac{\cosh^2(KH)}{\sinh(2KH)} \right\}. \quad (5.1.11)$$

Equation (5.1.11) for $|\sigma_o|$ was plotted in figure 13. As figure 13 shows there is excellent agreement between this modified theory and the experiment. It was, therefore, concluded that the horizontal fluid velocity at the surface was zero.

The question now is, why is there no horizontal, fluid velocity at the surface? According to Lamb and Levich (ref. 21 and 22) this may be due to an incompressible, insoluble, massless, surface film on the fluid. A surface film of this type acts as a thin metal plate would. The motion of fluid can easily bend the surface film, that is, cause the film to move vertically. The fluid motion cannot, however, cause the film to move horizontally because the film is incompressible. Because of the finite viscosity of the fluid the fluid at the surface must move with the film. This means that the fluid at the surface can move vertically but, because of the film's presence, cannot move horizontally. In other words, there can be no horizontal, fluid velocity at the surface if an incompressible, insoluble, surface film is present.

Lamb (ref. 21) considered theoretically the effect of an incompressible, insoluble, surface film for deep fluid waves. Van Dorn (ref. 14) too, considered this type of film. He worked theoretically and experimentally on progressive, gravity waves in a rectangular tank. Van Dorn claims to have calculated the total viscous damping coefficient including the surface film effect for all values of KH. This, unfortunately, is not true because his calculations use a formula taken from Landau and Lifshitz (ref. 44) which is only true for deep fluids (i. e. $KH \gg 1$). His experimental results do not closely agree with his theory.

Surface film effects were discussed theoretically as a function of the compressibility and solubility of the film by Levich and Dorrestein (ref. 22 and 24) for deep fluid waves (i. e. $KH \gg 1$). Experimental work to investigate these effects for deep fluid, capillary waves was carried out by Davies and Vose (ref. 16). Their experiments demonstrated, in agreement with theory, that damping is increased by factors of two or three by surface films. Only when the experimental equipment and fluid

were scrupulously cleaned did the damping coefficient agree with theoretical calculations which neglected surface film effects.

It can be concluded from our work that the observed viscous damping coefficients agree with the linear theory when the assumption that the flow is irrotational at the fluid surface is replaced with the assumption that there is no horizontal, fluid velocity at the surface. Also, the comments and work of others in the field suggest that an incompressible, insoluble, surface film made this latter assumption valid during our experiments.

This concludes the study of surface waves free of magnetic fields. In the following two chapters the effect of a vertical, magnetic field is theoretically and experimentally studied.

CHAPTER 6

THEORETICAL CALCULATION OF MAGNETIC DAMPING OF SURFACE WAVES FOR LOW MAGNETIC REYNOLDS NUMBERS

In this chapter the damping coefficient is derived for standing, axisymmetric, surface waves on an ideal, incompressible fluid of finite conductivity and depth in a vertical, uniform, constant, applied magnetic field, B_3 . The theory in this chapter was developed to explain the results of the experiment described in chapter 7. A more general discussion of damping by magnetic fields is made in appendix 3.

Figure 14 shows the nature of the problem to be solved. We define the following:

$\hat{B}$ = magnetic field.
$\hat{E}$ = electric field.
σ = electrical conductivity of the fluid.
$\hat{J}$ = current density.
$\hat{v}$ = fluid velocity.
ρ = fluid density
ζ = surface wave amplitude.
H = fluid depth.
A = radius of fluid container.
T = fluid surface tension.
P = pressure.
B_3 = applied magnetic field.
g = gravitational constant.
k = radial wave number of the surface wave.
ν = fluid viscosity.

We use the following assumptions and equations:

Maxwell's equations (assuming no free charge)

$$\hat{\nabla}\cdot\hat{B} = 0$$
$$\frac{\partial \hat{B}}{\partial t} = -\hat{\nabla}\times\hat{E}$$
$$\hat{\nabla}\times\hat{B} = \mu\hat{J} + \mu\epsilon\frac{\partial\hat{E}}{\partial t} \qquad (6.1.1)$$
$$\hat{\nabla}\cdot\hat{E} = 0$$

(The above equations give $\hat{\nabla}\cdot\hat{J} = 0$.)

Ohm's law (neglecting Hall currents)

$$\hat{J} = \sigma(\hat{E} + \hat{v}\times\hat{B}) \qquad (6.1.2)$$

In this work we make the assumption that the magnetic Reynolds number, Rm, is much less than one. ($Rm = \mu\sigma V\ell$ where V and ℓ are the characteristic

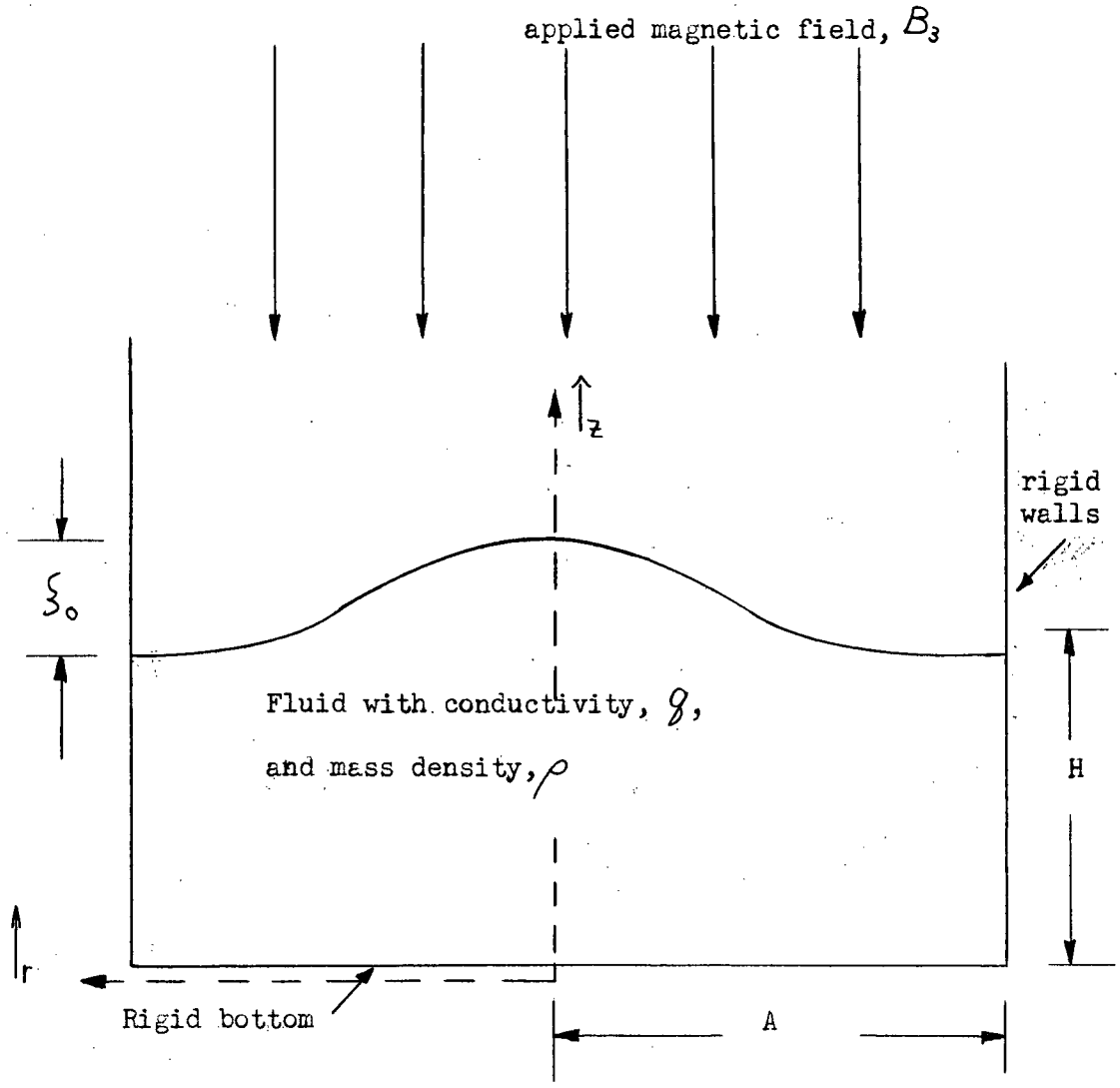

Figure 14. Description of the magnetic damping problem to be solved.

velocity and length, respectively). This means that $\hat{E} \ll \hat{V} \times \hat{B}$ in equation (6. 1. 2) and that the induced magnetic field, $\delta\hat{B}$, is much smaller than the applied magnetic field, B_3.

The fluid equations are

$$\frac{\partial \rho}{\partial t} + \hat{\nabla}\cdot(\rho\hat{v}) = 0 \qquad (6.1.3)$$

and $$\rho\left\{\frac{\partial \hat{v}}{\partial t} + (\hat{V}\cdot\hat{\nabla})\hat{V}\right\} = -\hat{\nabla}P - \rho\hat{\nabla}G + \hat{J}\times\hat{B} + \nu(\text{other terms}) \qquad (6.1.4)$$

we assume $\nu = 0$ (i. e. ideal fluid),

that ρ is a constant (i.e. incompressible fluid),

and $G = gz$ (i.e. in a constant gravitational field).

The Linearity conditions required are

$$\left.\begin{aligned} &K\zeta \ll 1, \\ &\zeta/H \ll 1, \\ \text{and}\quad &\zeta K \ll (HK)^3. \end{aligned}\right\} \qquad (6.1.5)$$

The boundary conditions are

$$\hat{V}\cdot\hat{n} = 0 \quad \text{(at rigid walls)}, \qquad (6.1.6)$$

$$P = P_0 - T\left(\frac{1}{r}\right)\frac{\partial}{\partial r}\left(\frac{r\,\partial\zeta}{\partial r}\right) \quad \text{(at the free surface)}, \qquad (6.1.7)$$

and $$V_z = \frac{\partial \zeta}{\partial t} \quad \text{(at the free surface)}. \qquad (6.1.8)$$

The surface wave is assumed to be axisymmetric. The problem will be solved using a perturbation technique. (i.e. we assume $\hat{B} = \hat{B}_3 + \delta\hat{B}$ where $|\delta\hat{B}| \ll |\hat{B}_3|$.) The oscillation frequency, f, and the damping coefficient, σ_B, are found by assuming that the time dependence is of the form $\exp(-int)$ where $n = 2\pi f + i\sigma_B$. Fraenkel (ref. 24) has solved this problem with the restriction $KH \ll 1$. We will solve this problem for all values of KH.

By using (6. 1. 5) in (6. 1. 4), taking the curl curl of (6. 1. 4), dropping terms of first order or higher in $\delta\hat{B}/B_3$, and using (6. 1. 3) we find that

$$\rho n \left\{ \frac{\partial}{\partial z} \left(-\frac{\partial V_z}{\partial z} \right) - \frac{1}{r} \frac{\partial}{\partial r} \left(r \frac{\partial V_z}{\partial r} \right) \right\} = g B_3^2 \frac{\partial V_z}{\partial z^2} . \qquad (6.1.9)$$

We recall that

$\frac{1}{r} \frac{\partial}{\partial r} \left\{ r \frac{\partial}{\partial r} J_o (Kr) \right\} = -K^2 J_o (Kr)$ (where Jo (Kr) is a Bessel function of order 0). Therefore, we can use

$V_z \propto$ Jo (Kr) $\{A_1 \cosh (\hat{k} z) + A_2 \sinh (\hat{k} z)\}$ as a solution to (6.1.9). We note, however, that $A_1 = 0$ because a boundary condition (equation 6.1.6) gives us $V_z = 0$ at $z = 0$. Using V_z in (6.1.9) we find that

$$\hat{k}^2 \left(1 + \frac{i g B_3^2}{n \rho}\right) = K^2 . \qquad (6.1.10)$$

The value of K is found in the following manner. By taking the curl of (6.1.4) we find that $\frac{\partial V_r}{\partial z} \left\{ 1 + \frac{i g B_3^2}{n \rho} \right\} = \frac{\partial V_z}{\partial r}$. Therefore, $V_r \propto$ Jo$'$ (Kr). The boundary condition at the walls gives us $V_r = 0$ at $r = A$.

Therefore, $J_o' (KA) = 0$. (6.1.11)

The value of K, as a result, is determined by the roots of J_o' .

The dispersion relation (relating n to K, $\hat{k}$, B_3 , H etc.) is found by taking the time derivative of (6.1.4) and evaluating its z component at the surface. Note that the $\hat{J} \times \hat{B}$ term in the z component of equation (6.1.4) is of the order of $V_z g B_3 \delta B$ and, therefore, can be neglected. This gives $\rho \ddot{V}_z = \frac{T}{r} \frac{\partial}{\partial r} \left(r \frac{\partial \dot{\xi}}{\partial r} \right) - \rho g \frac{\partial \dot{\xi}}{\partial z}$. (6.1.12)

We recall that $\dot{\xi} = V_z$ at the surface. This means that $\xi \propto$ Jo $(Kr) e^{-int}$. We define ψ so that $\frac{\partial \psi}{\partial z} = V_z$. Therefore (6.1.12) becomes

$$n^2 \rho \frac{\partial \psi}{\partial z} = (TK^2 + g\rho) \frac{\partial^2 \psi}{\partial z^2} \text{ (evaluated at } z = H). \qquad (6.1.13)$$

However, $\psi \propto \cosh (\hat{k} z)$ because $\frac{\partial \psi}{\partial z} = V_z \propto \sinh (\hat{k} z)$.

As a result, (6. 1. 13) becomes

$$n^2 = \left\{ \frac{TK^2}{\rho} + g \right\} \hat{k} \tanh (\hat{k} H) \qquad (6.1.14)$$

The problem is solved, therefore, by considering the three equations, (6. 1. 14), (6. 1. 11) and (6. 1. 10). They are as follows:

$$\left.\begin{aligned} n^2 &= \left\{ \frac{TK^2}{\rho} + g \right\} \hat{k} \tanh (\hat{k} H) \\ \hat{k}^2 \left(1 + i \frac{g B_3^2}{n \rho}\right) &= K^2 \\ J'_o (KA) &= 0 \end{aligned}\right\} \qquad (6.1.15)$$

where $n = 2\pi f + i\sigma_B$ and $\zeta \propto J_o (Kr) e^{-int}$.

For $B_3 = 0$ the above results agree with Coulson (ref. 6). The problem of finding n in terms of K, H, and B_3 is simplified if we assume $\frac{g B_3^2}{\rho |n| / \sigma_B} \ll 1$. It is clear later that this corresponds to assuming that $\sigma_B / 2\pi f \ll 1$. This assumption is consistent with the experimental results described in chapter 7. Using the above assumption and using the fact

$$\tanh\{A (1 + i\Theta)\} \simeq \{\tanh (A)\}\left\{1 + \frac{4A\Theta i}{(1 + A^2\Theta^2)(e^{2A} - e^{-2A})}\right\} \text{ for } \Theta \ll 1$$

we find that (6. 1. 15) reduces to

$$\left.\begin{aligned} n &= 2\pi f + i\sigma_B \\ (2\pi f)^2 &= \left\{ \frac{TK^3}{\rho} + gK \right\} \tanh (KH) \\ \sigma_B &= \frac{-B_3^2 g}{4\rho} \left\{ 1 + \frac{4KH}{e^{2KH} - e^{-2KH}} \right\} \\ J'_o (KA) &= 0 \\ \zeta &\propto J_o (Kr) e^{-int} \end{aligned}\right\} \qquad (6.1.16)$$

The interesting points to note are the following:

(i) f is independent of B_3 for all KH.

(ii) σ_B is proportional to $\frac{B_3^2 g}{\rho}$ for all KH.

(iii) For $KH \gg 1$ $\sigma_B = -\frac{B_3^2 g}{4\rho}$.

(iv) For $\kappa H \ll 1$ $\sigma_B = \frac{-B_3^2 q}{2\rho}$. This agrees with the theoretical calculation by Fraenkel (ref. 24).

(v) The shape of the wave is independent of B_3.

In the next chapter the results of the experiment to test this theory are given. f and σ_B were measured for different values of B_3, κ, and H. The experimental results agree well with the above theoretical calculations.

7 The problem of solving (6. 1. 15) for all values of $\frac{qB_3^2}{\rho n}$ was not considered.

CHAPTER 7

EXPERIMENTAL STUDY OF THE MAGNETIC DAMPING OF A SURFACE WAVE IN MERCURY

This chapter describes the experimental study of the magnetic damping coefficient, σ_B, of linear, gravity, standing, surface waves in mercury immersed in an applied, vertical, uniform, constant, magnetic field, B_3. The microwave cavity technique was used to investigate the relations between σ_B, H, K, and B_3. A discussion of the results and a comparison with the theory (developed in chapter 6) is also included in this chapter.

The values of σ_B were found from the measurement of the observed, total damping coefficient, σ, by assuming $\sigma = \sigma_o + \sigma_B$. The values of σ_o that were used here were obtained from the experiment described in Chapter 5. The results are summarised in figure 15, A, B and C. This experiment studied both deep and shallow fluid waves. KH was varied from about 0.4 to about 4.0. In figure 15 the magnetic field values are described as, for example, "approx. 2100 gauss." This means that the magnetic field value was in the 2100 gauss range (i.e. between 2050 and 2150 gauss). The measured value with an error of less than 5% was used, however, to calculate σ_B / B_3^2.

The linearized theory of standing waves in a vertical, magnetic field has been developed in chapter 6 for this experiment. Equation (6. 1.16) gives

$$\sigma_B = -\frac{\rho B_3^2}{4\rho} \left\{ 1 + \frac{4KH}{\exp(2KH) - \exp(-2KH)} \right\} \qquad (7.\ 1.\ 1)$$

The assumptions used to develop this theory are summarized in table 1. The above equation was used to plot σ_B as a function of depth with wavelength as a parameter (figure 15 A, B, C). The plots show that the agreement between the theory and the experiment is very good. Any difference can be explained by the experimental error in measuring σ_B and B_3^2. The

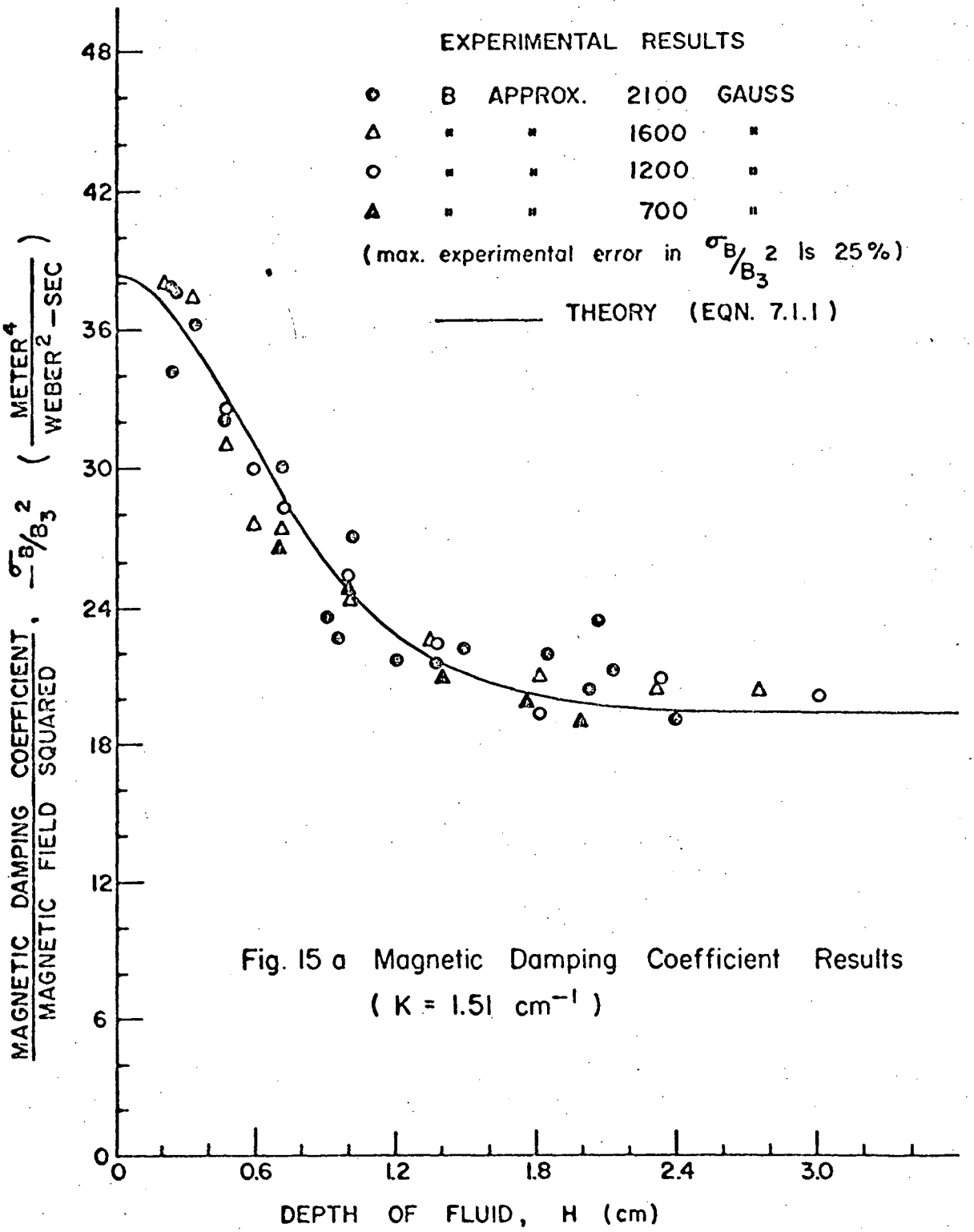

Fig. 15 a Magnetic Damping Coefficient Results
(K = 1.51 cm^{-1})

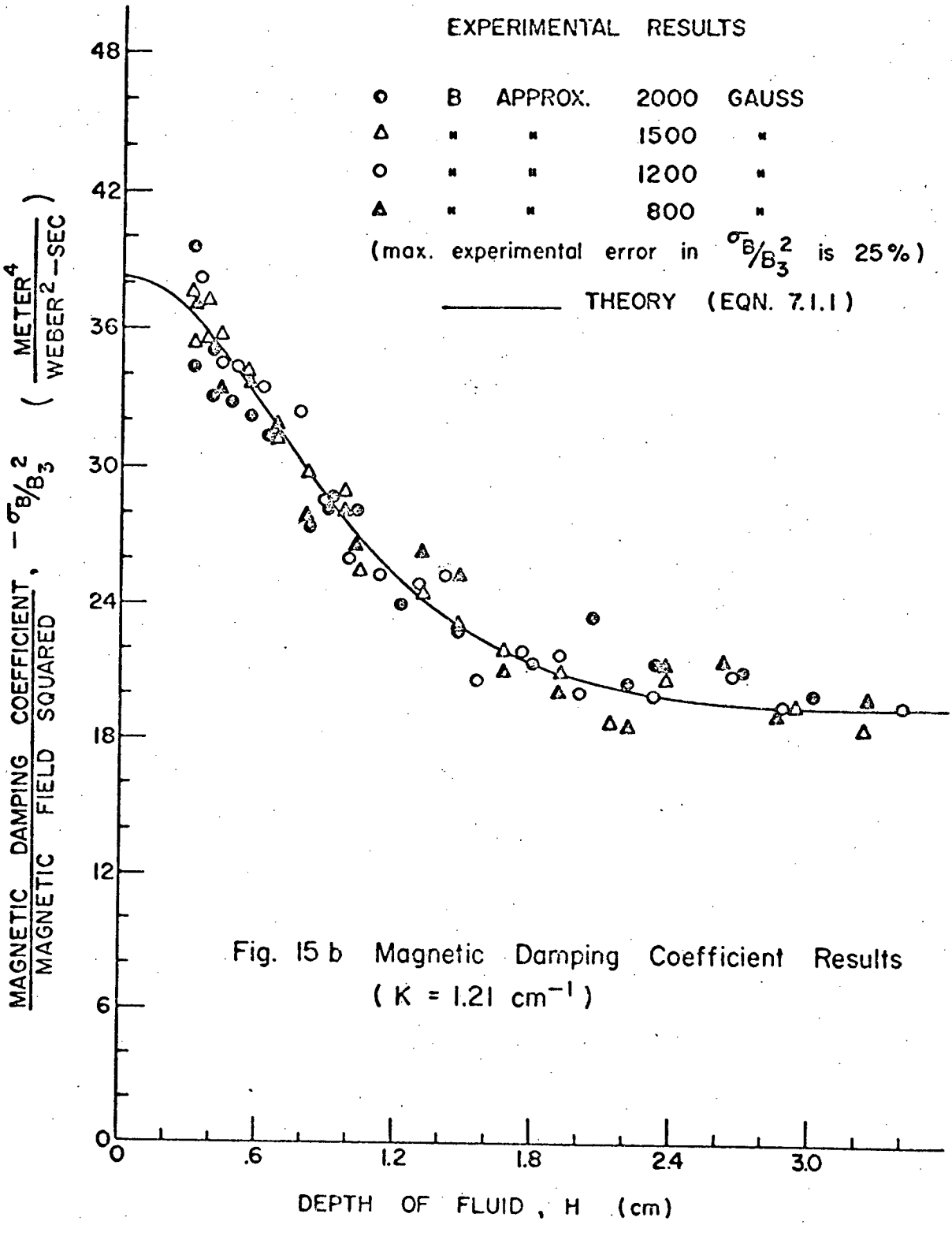

Fig. 15 b Magnetic Damping Coefficient Results
(K = 1.21 cm^{-1})

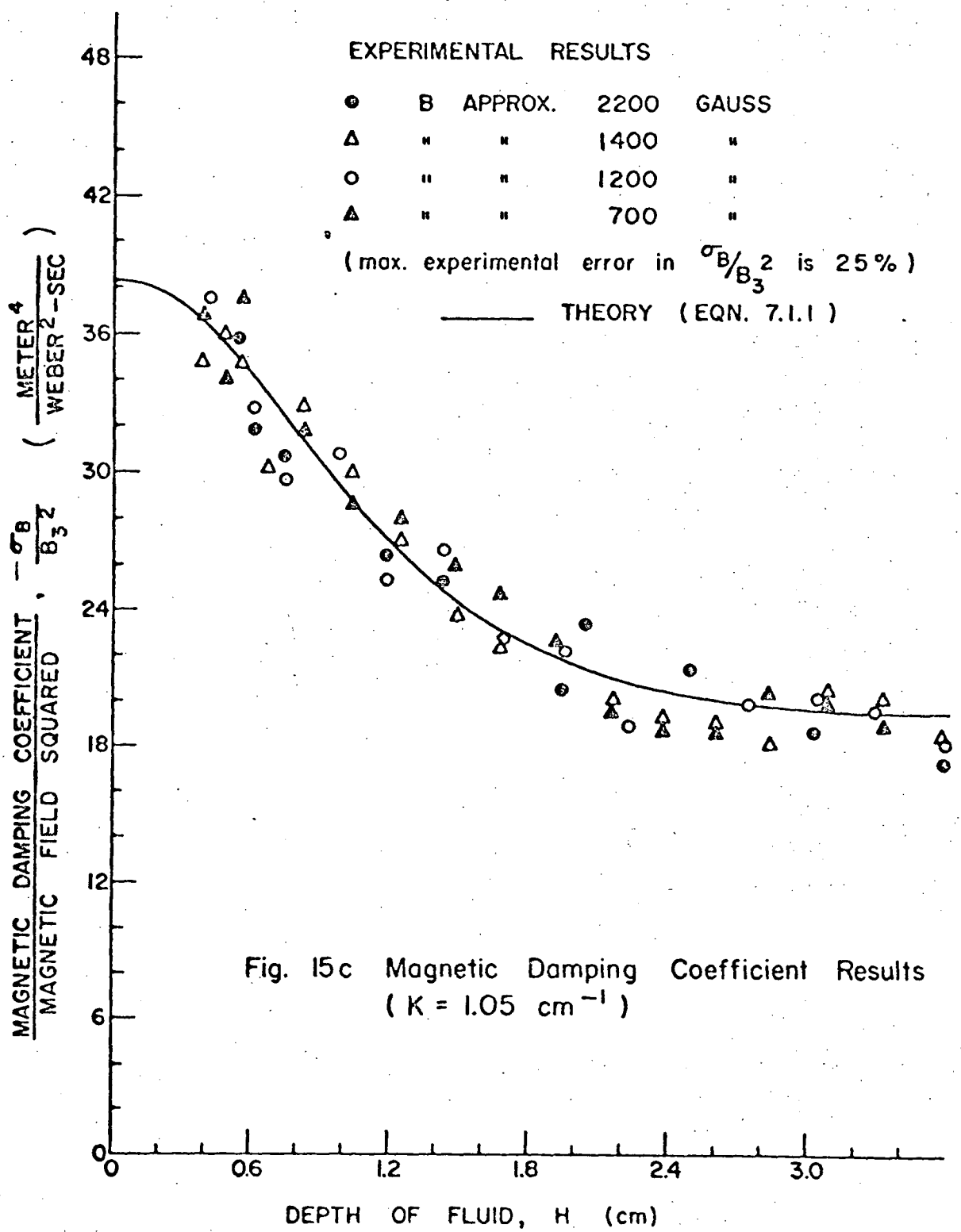

Fig. 15c Magnetic Damping Coefficient Results
(K = 1.05 cm^{-1})

percent error in the measurement of σ_B could be as high as 15% and the percent error in the measurement of B_3^2 could be as high as 10%.

The oscillation frequency, f, was found to be independent of B_3 to within 1%. This agrees with the theory developed in chapter 6.

CHAPTER 8 FUTURE WORK

It is the intention of this chapter to list a number of questions which arise naturally from the work reported in this thesis. The answering of these questions is regarded as future work.

The microwave cavity technique has proved very useful for studying the viscous and magnetic damping of a surface wave on a conducting fluid. Can it also be used to study surface motion caused by density gradients, temperature gradients, and current discharges in a conducting fluid?

In appendix I the theory for the use of a rectangular microwave cavity as an automatic Fourier analyser of surface waves was developed. Can this theory be put into practise?

In chapter 4 it was suggested that the observed oscillation frequency of a standing surface wave was larger than that predicted by the standard theory because of the meniscus. Can a detailed theory be developed to account for this effect?

In chapter 5 experimental evidence indicated that there was no horizontal motion of the surface when the viscous damping of a surface wave on mercury was studied. Was this due to an incompressible, insoluble, surface film? Could an oil or mercury oxide film have caused this effect? Could the em. fields in the microwave cavity have caused this effect?

In chapter 6 and appendix 3 a theory for the magnetic damping of surface waves was developed by using the restrictions $Rm \ll 1$ and $(\sigma B^2)/(m/\rho) \ll 1$ (i.e. $\sigma_B / 2\pi f \ll 1$). Can a theory be developed without these restrictions? What would we expect if $Rm \gg 1$ or if $(\sigma B^2)/(m/\rho) \gg 1$?

As chapter 7 shows, the experiment on the damping of a surface wave by a vertical magnetic field confirms the theory that was developed for it. Will a similar experiment using a horizontal magnetic field agree with the theory developed in appendix 3?

SUMMARY

A new, convenient method of studying small amplitude, surface waves has been developed theoretically and experimentally. This method is free of the problems associated with immersion devices. It is capable of measuring surface waves where $\zeta_0 K \geq 10^{-4}$. In certain cases it can be used to automatically Fourier analyse arbitrary surface waves.

This method was used to study a simple, axisymmetric surface wave in liquid mercury. The wave was studied for values of KH between 0.4 and 4.0. Experiments showed that the oscillation frequencies of the wave were higher than predicted by the linear theory by up to 15%. It was suggested that this discrepancy can be accounted for by considering the effect that the meniscus has upon the boundary condition at the walls. Experiments also showed that the viscous damping coefficient was much higher than predicted by standard theory. In view of this the author computed the additional damping coefficient which resulted when the assumption that "the flow is irrotational at the fluid surface" was replaced by the assumption that "the horizontal fluid velocity is zero at the surface." This additional term was found to be $-\sqrt{\frac{\nu 2\pi\zeta}{2}}\, K\, \frac{\cosh^2(KH)}{\sinh(2KH)}$. The experimental results were in excellent agreement with the theory when this effect was included.

Finally, the damping of surface waves by a vertical magnetic field was considered for low magnetic Reynolds Numbers. The magnetic damping coefficient and the oscillation frequency were calculated by the author for an axisymmetric, linear, standing surface wave on an incompressible, electrically conducting fluid. Detailed calculations were made for the case $\frac{\sigma B_0^2}{\rho 2\pi\zeta} \ll 1$. They showed that the oscillation frequency was independent of the magnetic

field and that the magnetic damping coefficient was given by $-\frac{\sigma B_3^2}{4\rho}\left\{1+\frac{4kH}{\exp(2kH)-\exp(-2kH)}\right\}$. An experiment with liquid mercury was performed. The results are in excellent agreement with the above calculation.

REFERENCES

1. Langmuir, R. V. (1961), Electromagnetic fields and Waves, McGraw-Hill series in Engineering Sciences

2. Slater, J. C. (1963), Microwave Electronics, Bell Laboratories Series

3 Ginzton, E. L. (1957), Microwave Measurements, McGraw-Hill Book Company, Inc. p. 445

4 Whitmer, R. M. (1962), Electromagnetics, Prentice-Hall, Inc.

5 Morse, P. M. and Feshback, H. (1953), Methods of Theoretical Physics, McGraw-Hill Book Company, Inc. p. 1565

6 Coulson, C. A. (1961), Waves, University Mathematical Texts.

7 Case, K. M. and Parkinson, W. C. (1956), J. of Fluid Mech. 2, 172

8 Tadjbakhsh, I. and Keller, J. B. (1959), J. of Fluid Mech. 8, 442

9 Rayleigh, Lord (1890), Phil. Mag. XXX, 386

10 Keulegan, G. H. (1958), J. of Fluid Mech. 6, 33

11 Fultz, D. (1962), J. Fluid Mech. 13, 193

12 Taylor, Sir G. (1953), Proc. Roy. Soc. A, 218, 44

13 Ursell, F. (1953), Proc. Cam. Phil. Soc. 49, 685

14 Van Dorn, W. G. (1965), J. Fluid Mech. 24, 769

15 Kranzer, H. C. and Keller, J. B. (1959), J. Appl. Phys. 30, 398

16 Davies, J. T. and Vose, R. W. (1965), Proc. Roy. Soc. A, 286, 218

17 Grosch, G. C. and Ward, L. W. and Lukasik, S. J. (1960), Phys. of Fluids 3, 477

18 Hunt, J. M. (1963), Phys. Fluids 7, 156

19 Spies, R. (1958), Aerojet - General Corporation Rept. 1508

20 Eagleson, P. S. (1959), M. I. T. Hydrodynamics Laboratory Technical Rept. No. 32

21 Lamb, H. (1945), Hydrodynamics, Dover Publications, Inc., New York.

22 Levich, V. G. (1941), Acta Physicochim. U.S.S.R. 14, 307, 321; Physicochimical Hydrodynamics, New Jersey: Prentice-Hall Inc. (1962).

23 Dorrestein, R. (1951), Proc. Acad. Sci. Amst. B, 54, 260, 350

24. Fraenkel, L. E. (1959), J. of Fluid Mech. 7, 81

25 Levich, V. G. and Gurevich, Yu. Ya. (1962) Dokl. Akad. Nauk. S. S. S. R. 143, 64

26 Roberts, P. H. and Boardman, A. D. (1962), Astrophys. J. (U.S.A.) 135, 552

27 Wentzell, R. A. and Blackwell, J. H. (1965), Can. J. of Physics, 43, 645

28 Kukshas, B. and Ilgunas, V. and Barshauskas, K. (1961), Litov. Fiz. Sbornik (U.S.S.R.) 1, 135.

29 Gupta, A. S. (1964), Proc. Roy. Soc. A (G. B.) No. 1374, 214

30 Vandakurov, Yu, V. (1963), Soviet Physics - Technical Physics (U. S. A.) 2, 104.

31 Peskin, R. L. (1963), Phys. of Fluids (U. S. A.) 6, 643

32 Nayyar, N. K. and Trehan, S. K. (1963) Phys. of Fluids (U.S.A.) 6, 1587

33 Murty, G. S. (1963), Ark. Fys. (Sweden) 24, 529

34 Bickerton, R. J. and Spalding, I. J. (1962), Plasma Phys. - Accelerators - Thermonuclear Res. (G. B.) 4, 151.

35 Dattner, A. (1962), Ark. Fys. (Sweden) 21, 71.

36 Murty, G. S. (1961), Ark. Fys. (Sweden), 19, 483

37 Tandon, J. N. and Talwar, S. P. (1961), Plasma Phys. - Accelerators - Thermonuclear Res. (G. B.) 3, 261

38 Lehnert, B. and Gjögsen, G. (1960), Rev. Mod. Phys. (U. S. A.) 32, 813.

39 Curzon, F. L. and Howard, R. (1961), Can. Journal of Physics 39, 1901

40 Curzon, F. L. Howard, R. and Powell, E. R. (1962), J. of Electronics and Control 14, 513

41 Tucker, M. J. and Charnock, H. (1955), Proc. Fifth Conf. Coastal Engineering (University of California, Berkeley).

42 Morrison, J. R. (1949), Bull. Beach Erosion Bd. 3, 16

43 Wiegel, R. L. (1947), University of California Wave Project Report No. HE 116 - 269 (Berkeley).

44 Landau, L. D. and Lifshitz, E. M. (1959), Fluid Mechanics, Ch. 6 Reading, Mass: Addison-Wesley

45 Winsor, F. and Parry, M. (1963), The Space Child's Mother Goose, Simon and Schuster, Inc.

APPENDIX I CALCULATION OF THE RESONANT FREQUENCY CHANGE FOR A SURFACE WAVE IN A RECTANGULAR CAVITY

The method for calculating the change in resonant frequency of a microwave cavity for a surface perturbation on the end plate of the cavity is the same as that in chapter 2. Details of the cavity are given in figure 16.

In a rectangular cavity it can be shown (ref. 1) that

$$\hat{E} = (E_x \hat{i}_x + E_y \hat{i}_y + E_z \hat{i}_z) e^{j\omega t} \quad \text{and} \quad \hat{B} = (B_x \hat{i}_x + B_y \hat{i}_y + B_z \hat{i}_z) e^{j\omega t} \tag{A. 1. 1}$$

where

$$E_x = E_1 \cos(\ell\pi x/A) \operatorname{Sin}(m\pi y/B) \operatorname{Sin}(n\pi z/L)$$

$$E_y = E_2 \operatorname{Sin}(\ell\pi x/A) \cos(m\pi y/B) \operatorname{Sin}(n\pi z/L)$$

$$E_z = E_3 \operatorname{Sin}(\ell\pi x/A) \operatorname{Sin}(m\pi y/B) \cos(n\pi z/L)$$

$$B_x = -\frac{j}{\omega}\left[\frac{E_3 m\pi}{B} - \frac{E_2 n\pi}{L}\right] \operatorname{Sin}(\ell\pi x/A) \cos(m\pi y/B) \cos(n\pi z/L)$$

$$B_y = -\frac{j}{\omega}\left[\frac{E_1 n\pi}{L} - \frac{E_3 \ell\pi}{A}\right] \cos(\ell\pi x/A) \operatorname{Sin}(m\pi y/B) \cos(n\pi z/L)$$

$$B_z = -\frac{j}{\omega}\left[\frac{E_2 \ell\pi}{A} - \frac{E_1 m\pi}{B}\right] \cos(\ell\pi x/A) \cos(m\pi y/B) \operatorname{Sin}(n\pi z/L)$$

$$\frac{\ell\pi E_1}{A} + \frac{m\pi E_2}{B} + \frac{n\pi E_3}{L} = 0$$

where E_1, E_2 and E_3 are the peak values of E_x, E_y and E_z and where

$$\omega^2 \epsilon\mu = \left(\frac{\ell\pi}{A}\right)^2 + \left(\frac{m\pi}{B}\right)^2 + \left(\frac{n\pi}{L}\right)^2. \tag{A. 1. 2}$$

In order to specify completely $\hat{E}$ and $\hat{B}$ (except for the arbitrary power factor) it is necessary to let either $E_3 = 0$ (T. E. modes) or $B_z = 0$ (T. M. modes).

In reference 6 it is shown that the amplitude of a linear, standing surface wave on an ideal, incompressible fluid in a rectangular tank can be expressed by $\zeta = \sum_{S,P} \zeta_o(S,P) \cos\frac{(P\pi x)}{A} \cos\frac{(S\pi y)}{B}$ (see fig. 16). S and P are integers. The calculation for $2\left(\frac{\omega_a - \omega}{\omega}\right)$ will be made assuming

that only one simple standing wave is present

(i.e. $\zeta = \zeta_0 \cos\left(\frac{P\pi x}{A}\right) \cos\left(\frac{S\pi y}{B}\right)$). By using equation (A 1.1) in

(1. 1. 1) it is easy to show

$$N_E^2 = \frac{ABL}{8}\Big\{ E_1^2 (1-\delta_{m,0})(1-\delta_{n,0})(1+\delta_{l,0}) + E_2^2 (1-\delta_{l,0})\times$$

$$(1-\delta_{n,0})(1+\delta_{m,0}) + E_3^2 (1-\delta_{m,0})(1-\delta_{l,0})(1+\delta_{n,0})\Big\}$$

and $N_B^2 = \epsilon\mu N_E^2$. (A1.3)

As before, if the amplitude of the surface wave, ζ_0, is small

(i.e. $\frac{n\pi\zeta_0}{L} \ll 1$) and $\frac{\omega_a - \omega}{\omega} \ll 1$ then $\frac{\omega_a - \omega}{\omega}$ can be calculated

from

$$2\left(\frac{\omega_a-\omega}{\omega}\right) = \frac{\zeta_0 AB}{\omega^2 N_B^2 \pi^2}\left[\frac{E_3\pi m}{B} - \frac{E_2 n\pi}{L}\right]^2\left(\frac{\pi}{4}\right) D_1(l,P)\left(\frac{\pi}{4}\right) D_2(m,S)$$

$$+ \frac{\zeta_0 AB}{\omega^2 N_B^2 \pi^2}\left[\frac{E_1 n\pi}{L} - \frac{E_3 l\pi}{A}\right]^2\left(\frac{\pi}{4}\right) D_1(m,S)\frac{\pi}{4} D_2(l,P)$$

$$- \frac{\zeta_0 AB}{N_E^2 \pi^2} E_3^2\left(\frac{\pi}{4}\right)\left(\frac{\pi}{4}\right) D_1(l,P)\, D_1(m,S) \qquad \text{(A1. 4)}$$

where

N_B^2 and N_E^2 are given by equation (A1. 3), $\frac{l E_1}{A} + \frac{m E_2}{B} + \frac{n E_3}{L} = 0$,

and either $E_3 = 0$ (for T. E. modes) or

$\frac{l E_2}{A} - \frac{m E_1}{B} = 0$ (for T. M. modes).

Also, $\int_0^\pi \sin^2(i\theta)\cos(j\theta)\,d\theta = \frac{\pi}{4} D_1(i,j) = \begin{cases} 0 \text{ for } i = 0 \\ \frac{\pi}{2}(1-\delta_{i,0})\, j = 0 \\ -\frac{\pi}{4}\delta_{2i,j} \quad i \neq 0 \text{ and } j \neq 0 \end{cases}$

$$\int_0^\pi \cos^2(i\theta)\cos(j\theta)\,d\theta = \frac{\pi}{4} D_2(i,j) = \begin{cases} \pi\delta_{j,0} & i = 0 \\ \frac{\pi}{2}(1+\delta_{2i,0})\, j = 0 \\ \frac{\pi}{4}\delta_{2i,j} \quad i \neq 0 \text{ and } j \neq 0 \end{cases}$$

Therefore, if an em. wave is set up in the cavity such that $\ell = 0$ and $m \neq 0$ then $\frac{\omega_a - \omega}{\omega} \backsimeq 0$ unless $P = 0$ and $S = 2m$. (In other words, $\frac{\omega_a - \omega}{\omega}$ is proportional to the $P = 0$, $S = 2m$, Fourier component of the surface wave in the cavity). Similarly, if $m = 0$ and $\ell \neq 0$ then $\frac{\omega_a - \omega}{\omega} \backsimeq 0$ unless $S = 0$ and $P = 2\ell$. (In other words, $\frac{\omega_a - \omega}{\omega}$ is proportional to the $S = 0$, $P = 2\ell$, Fourier component of the surface wave in the cavity). This allows the "$P = 0$, $S = 2m$" and "$S = 0$, $P = 2\ell$ " Fourier components of an arbitrary surface wave to be studied with ease.

If an em. wave is set up in the cavity such that $\ell \neq 0$ and $m \neq 0$ then $\frac{\omega_a - \omega}{\omega} \backsimeq 0$ unless one or more of the following is true:

(i) $2\ell = P$ and $S = 0$

(ii) $2m = S$ and $P = 0$

(iii) $2\ell = P$ and $2m = S$.

In other words, em. modes of this type "react" to three different types of surface waves (i. e. three different Fourier components). In this case

$$\frac{\omega_a - \omega}{\omega} = C_1 \zeta_o(S = 0, P = 2\ell) + C_2 \zeta_o(S = 2m, P = 0) + C_3 \zeta_o(S = 2m, P = 2\ell)$$

where C_1, C_2 and C_3 are found from equation (1. 4. 2). Therefore, once $\zeta_o(S = 0, P = 2\ell)$ and $\zeta_o(S = 2m, P = 0)$ have been measured (by using the $\ell \neq 0$, $m = 0$ and $m \neq 0$, $\ell = 0$ em. modes) $\zeta_o(S = 2m, P = 2\ell)$ can be studied by the use of the $\ell \neq 0$, $m \neq 0$ em. modes.

In this way the rectangular microwave cavity can be used to automatically Fourier analyse an arbitrary, standing, surface wave in a rectangular tank.

APPENDIX 2 THE TEST OF SLATER'S THEOREM

A pie shaped perturbation (fig. 17) was introduced into the bottom of a microwave cavity to test Slater's theorem. The change in resonant frequency for such a perturbation was computed from the theorem in the same way as in chapter 2. The assumptions, $\frac{\omega_a - \omega}{\omega} \ll 1$ and $\frac{n\pi \delta_o}{L} \ll 1$, are used again.

It can be shown that for $\ell = 0$ (T. M. modes)

$$2\left(\frac{\omega_a - \omega}{\omega}\right) = \frac{K_o^2 \delta_o \phi}{N_B^2} \int_o^{R_1} \left[J_o'(K_o r)\right]^2 r dr - \frac{K_o^4 \omega^2 \delta_o \phi}{k^2 N_E^2} \int_o^{R_1} \left[J_o(K_o r)\right]^2 r dr. \quad \text{(A2.1)}$$

Similarly for $\ell \neq 0$

$$2\left(\frac{\omega_a - \omega}{\omega}\right) = \frac{K_o^2 \delta_o}{N_B^2 \ell 4} \left\{ 2\ell\phi + \sin(2\ell[\theta_1 + \phi]) - \sin(2\ell\theta_1) \right\} \int_o^{R_1} \left[J_\ell'(K_o r)\right]^2 r dr$$
$$+ \frac{\ell^2 \delta_o}{N_B^2 \ell 4} \left\{ 2\ell\phi - \sin(2\ell[\theta_1 + \phi]) + \sin(2\ell\theta_1) \right\} \int_o^{R_1} \frac{J_\ell^2(K_o r)}{r} dr$$
$$- \frac{\omega^2 k_o^4 \delta_o}{k^4 N_E^2 4} \left\{ 2\ell\phi + \sin(2\ell[\theta_1 + \phi]) - \sin(2\ell\theta_1) \right\} \int_o^{R_1} J_\ell^2(K_o r) r dr. \quad \text{(A2.2)}$$

N_B^2 and N_E^2 are given by equation (1. 3. 3).

It can be shown that for $\ell = 0$ (T. E. modes)

$$2(\omega_a - \omega)/\omega = \left(\frac{n\pi}{L}\right)^2 \frac{\delta_o \phi}{K^2 N_B^2} \int_o^{R_1} \left[J_o'(Kr)\right]^2 r dr. \quad \text{(A2.3)}$$

Similarly for $\ell \neq 0$

$$2\left(\frac{\omega_a - \omega}{\omega}\right) = \frac{\ell^2 \left(\frac{n\pi}{L}\right)^2 \delta_o}{4\ell K^4 N_B^2} \left\{ 2\ell\phi - \sin(2\ell\phi + 2\ell\theta_1) + \sin(2\ell\theta_1) \right\} \text{times}$$
$$\left\{ \int_o^{R_1} \frac{J_\ell^2(Kr)}{r} dr \right\}$$
$$+ \left(\frac{n\pi}{L}\right)^2 \frac{\delta_o}{K^2 N_B^2 4\ell} \left(2\ell\phi + \sin(2\ell\phi + 2\ell\theta_1) - \sin(2\ell\theta_1)\right) \text{times}$$
$$\left\{ \int_o^{R_1} \left[J_\ell'(Kr)\right]^2 r dr \right\}. \quad \text{(A2.4)}$$

N_B^2 is given by equation (1. 3. 4).

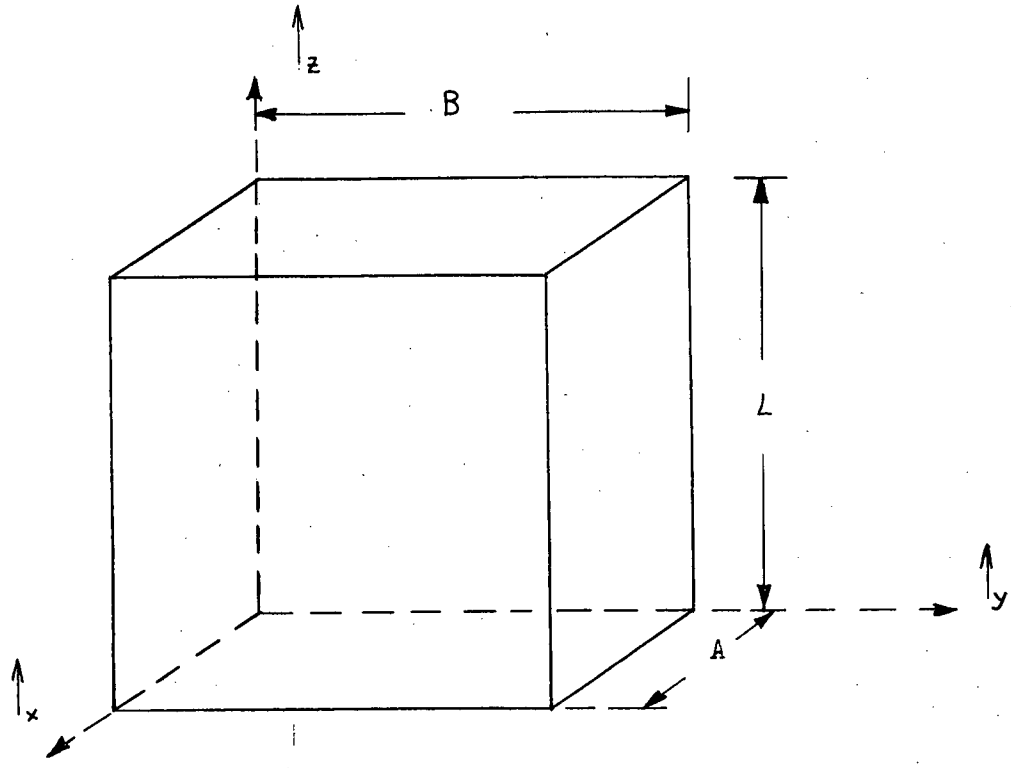

Figure 16 Rectangular microwave cavity

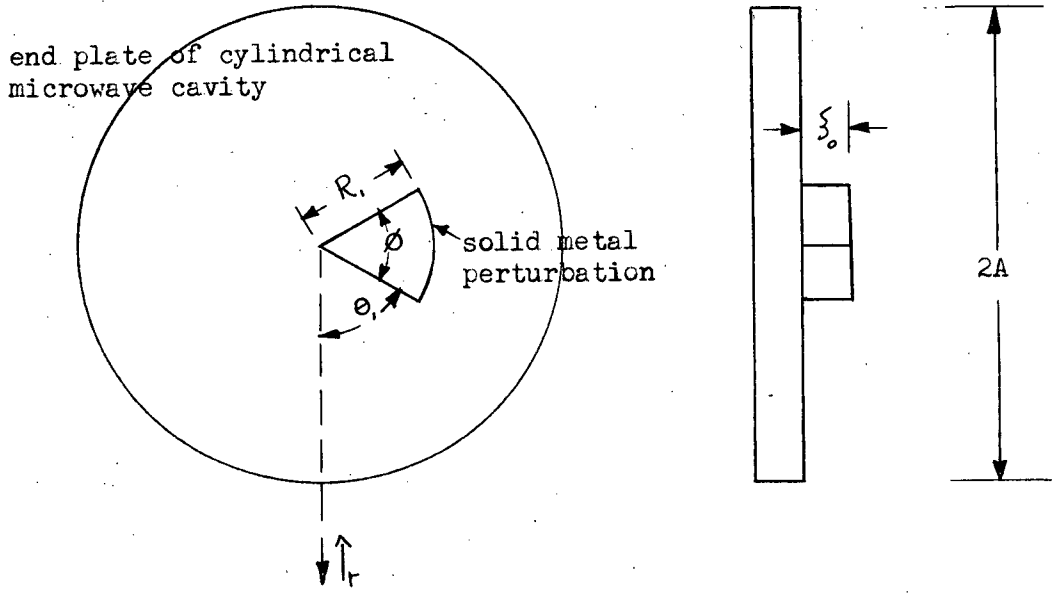

Figure 17 Details of the perturbation used to test Slater's theorem.

A pie shaped perturbation was placed on the bottom plate of the cavity. The azimuthal position, Θ_1, (see fig. 17) was varied. All other parameters were held constant. As the perturbation was rotated 360° about the axis of the cavity the resonant frequency varied from a minimum to a maximum a certain number of times. The difference between the maximum and the minimum resonant frequency, OF, and the number of variations, NO, were measured. Equation (A2.4) was used to calculate F and NO from Slater's theorem and a comparison was made between the theoretical and experimental values. This experiment was repeated for various L's (i.e. for different em. modes in the cavity). Equations (1. 2. 2) and (1. 2. 4) were used to identify the modes. The results are shown in table 2.

A similar experiment was performed but, in this case, the position of the perturbation was kept constant and the perturbation amplitude, S_o, was varied from 0 to .85 cm. All other parameters were held constant. The change in resonant frequency per change in perturbation amplitude, $\frac{\omega_a - \omega}{S_o 2\pi}$, was measured for $S_o \leq .4$ cm. Equation (A2.4) was used to calculate $\frac{\omega_a - \omega}{S_o 2\pi}$ from Slater's theorem. This experiment was repeated for various L's (i.e. for different em. modes in the cavity). The experimental results for the TE_{111} and TE_{211} modes are given in figure 18. It shows that, as expected, the change in resonant frequency is directly proportional to the amplitude of the perturbation. Table 3 shows that the experiment and theory are in agreement for the four modes that were tested.

Varying the size or position of the perturbation also resulted in small, undesirable changes in the length of the cavity. These unavoidable changes sometimes caused resonant frequency changes that were almost as large as those caused by changing the perturbation size or position. This effect can account for any difference between the theoretical and experimental values of tables 2 and 3.

Parameters for Table II (see figure 17)

$\delta_0 = .310$ cm. $\qquad \phi = 43^\circ$

$R_1 = 1.46$ cm $\qquad \frac{\omega}{2\pi} = 8.9$ KMc./s.

$A = 2.54$ cm.

Experiment			Theory					
L (cm.)	F (Gc./s.)	No	Mode	ℓ	m	n	F (Gc./s.)	No
1.83	.018	2	TE	1	1	1	.020	2
2.20	.008	4	TE	2	1	1	.006	4
4.45	.003	4	TE	2	1	2	.003	4

Table II. Comparison between theory and experiment

Parameters for Table III (see figure 17)

$R_1 = .97$ cm. $\qquad \phi = 43^\circ$

$A = 2.54$ cm. $\qquad \frac{\omega}{2\pi} = 8.9$ KMc./s

Experiment		Theory				
L (cm.)	$(\omega_a-\omega)/2\pi\delta_0$ (Gc/sec.cm.)	Mode	ℓ	m	n	$(\omega_a-\omega)/2\pi\delta_0$ (Gc/sec.cm.)
1.83	0.14	TE	1	1	1	0.15
2.20	0.017	TE	2	1	1	0.018
2.90	0.16	TM	1	1	1	0.12
3.66	0.071	TE	1	1	2	0.063

Table III. Comparison between theory and experiment.

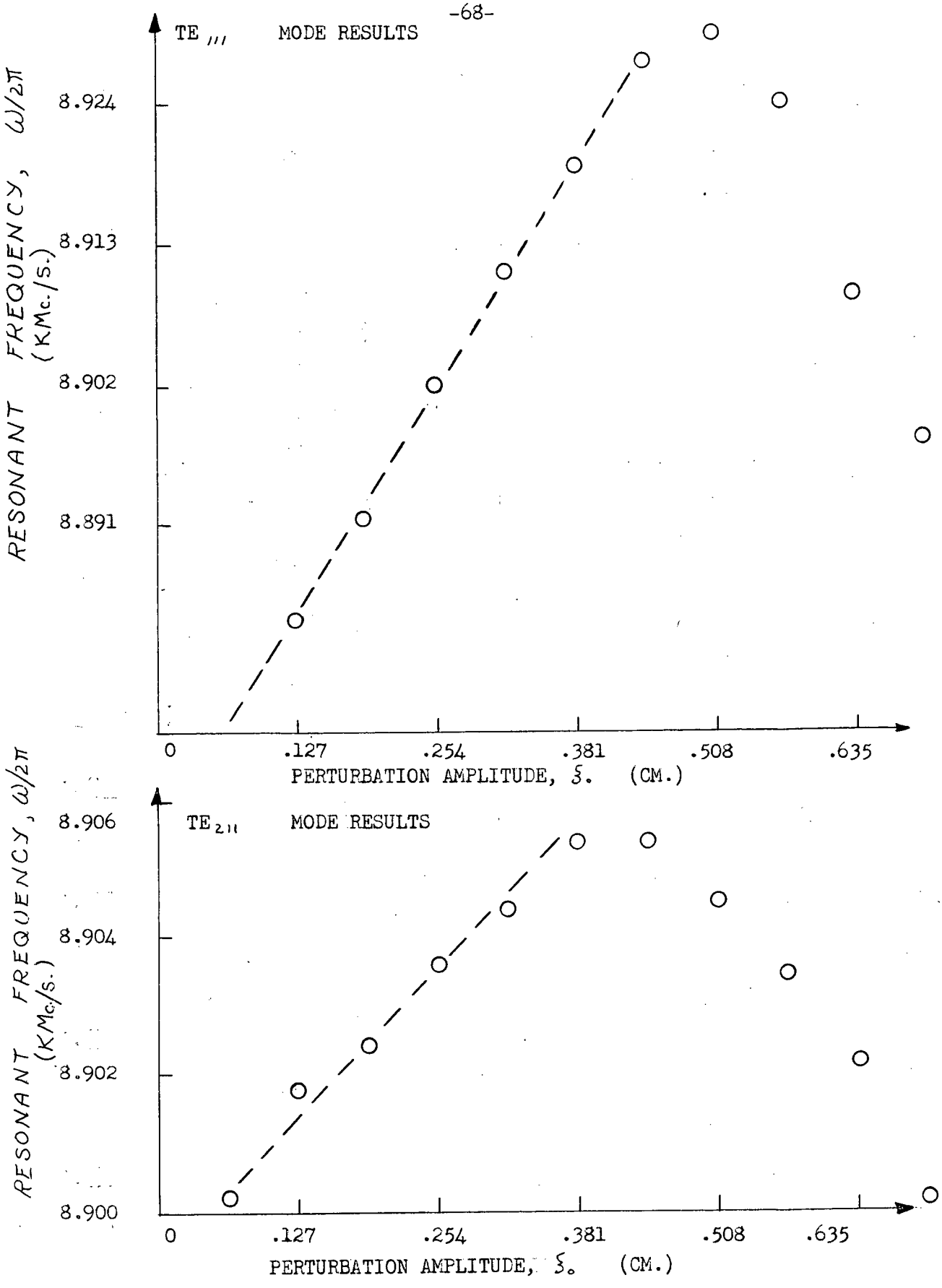

Fig. 18 Graphs showing the change in resonant frequency as a function of the perturbation amplitude.

In some cases when a perturbation was introduced into the cavity, two resonant frequencies were observed differing by less than 20Mc./s. The relative changes in these resonant frequencies, as the perturbation was being moved about in the cavity, suggested that they corresponded to identical em. modes (i.e. same l , m and n) with different azimuthal orientations.

As expected, the electromagnetic fields near a coupling hole or probe (between the waveguide and the cavity) were found to be different than given by equations (1. 2. 1) or (1. 2. 3). Probes were found to distort the fields in the cavity more than holes. A coupling hole, therefore, was used. It was made as small as possible and placed as far from the perturbation as possible (see fig. 5).

It was found in agreement with the theory that the change in resonant frequency was proportional to the perturbation amplitude for amplitudes less than .4 cm. When δ_0 was made greater than .4 cm., however, the change in resonant frequency was no longer proportional to δ_0 . This is to be expected because the small amplitude assumption that was made (i.e. $\frac{n\pi\delta_0}{L} \ll 1$) is not valid in this case.

The above results, therefore, show that Slater's theorem can be used to predict the change in resonant frequency of a microwave cavity caused by a small amplitude perturbation of the shape of that cavity.

APPENDIX 3

THEORETICAL CALCULATION OF THE MAGNETIC DAMPING OF SURFACE WAVES FOR LOW MAGNETIC REYNOLDS NUMBERS

In this appendix the damping coefficient is derived for linear, standing, surface waves on an ideal, incompressible fluid of finite conductivity and depth in a uniform, constant, applied magnetic field. Figure 19 shows the nature of the problem to be solved. The definitions are the same as those used in chapter 6 except that $k_1 = 2\pi/\lambda_1$ and $k_2 = 2\pi/\lambda_2$. The assumptions and equations (6. 1. 1), (6. 1. 2), (6. 1. 3), (6. 1. 4), and (6. 1. 5) in chapter 6 are used to solve the above problem. The boundary conditions are as follows:

$$V_z = 0 \quad \text{AT} \quad z = 0 . \tag{A3.6}$$

$$P = P_0 + T\left\{\frac{\partial^2 \xi}{\partial x^2} + \frac{\partial^2 \xi}{\partial y^2}\right\} \qquad \text{at the free surface.} \tag{A3.7}$$

$$V_z = \frac{\partial \xi}{\partial t} \qquad \text{at the free surface .} \tag{A3.8}$$

The problem will be solved using a perturbation technique. We assume $\hat{B} = \hat{B}_0 + \delta\hat{B}$ where $\delta\hat{B} \ll \hat{B}_0$. $\hat{B}_0$ is the applied magnetic field. $\hat{B}_0 = B_1 \hat{i}_x + B_2 \hat{i}_y + B_3 \hat{i}_z$. The oscillation frequency, f, and the damping coefficient, σ_B, are found by assuming that the time dependence is of the form $\exp(-int)$ where $n = 2\pi f + i\sigma_B$.

Frænkel (ref. 24) has solved this problem for the case $(k_1^2 + k_2^2)^{\frac{1}{2}} H \ll 1$, $B_1 = 0$, $B_2 = 0$. Roberts and Boardman (ref. 26) have solved it for the case $(k_1^2 + k_2^2)^{\frac{1}{2}} H \gg 1$, $B_1 = 0 = B_2$. Wentzell and Blackwell (ref. 27) have solved this problem for the case $k_1 H \gg 1$, $B_2 = 0 = B_3 = k_2$ and Kukshas, Ilgunas and Barshauskas (ref. 28) have considered various aspects of the case $B_3 = B_2 = k_2 = 0$. We will solve the problem for all values of $(k_1^2 + k_2^2)^{\frac{1}{2}} H$, k_1, k_2, B_1, B_2 , B_3 .

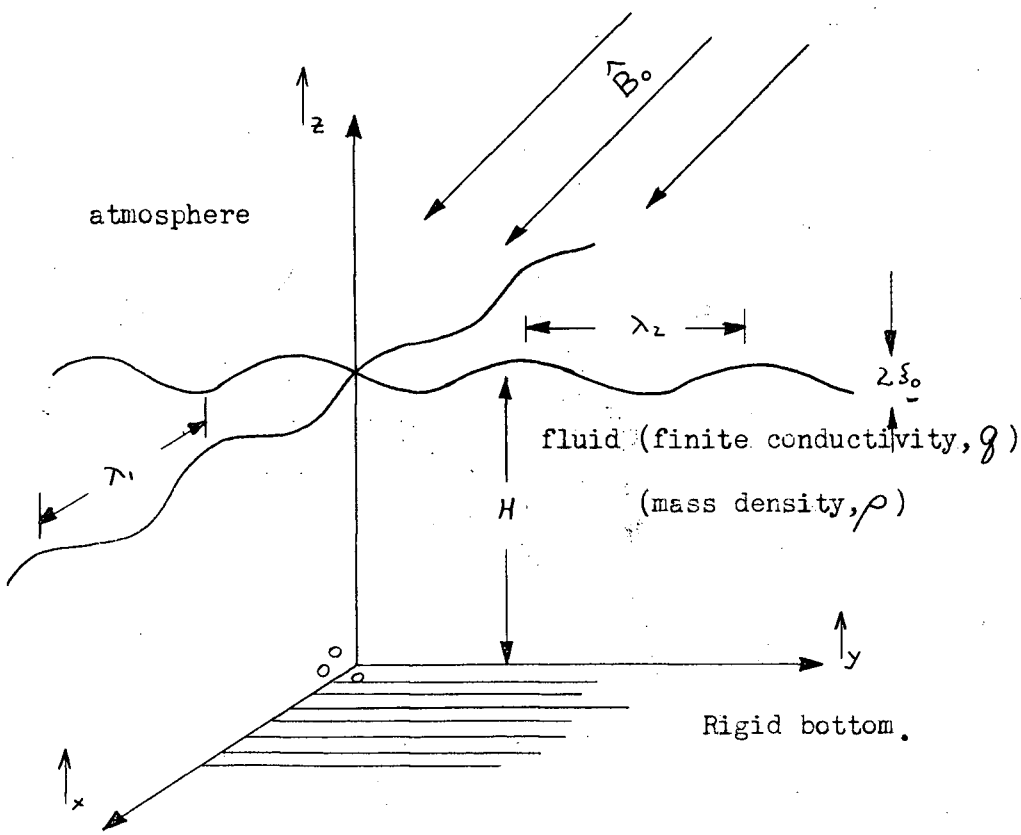

Fig. 19 Description of the magnetic damping problem to be solved.

By taking the curl curl of (6. 1. 4), dropping terms of second order or higher in $\frac{|\delta\hat{B}|}{B_0}$ and using the fact that $\hat{\nabla}\cdot\hat{V} = 0 = \hat{\nabla}\cdot\hat{B} = \hat{\nabla}\cdot\hat{J}$ we find that

$$i\eta\rho\nabla^2\hat{V} = g(\hat{B}_0\cdot\hat{\nabla})^2\hat{V}. \qquad (A\,3.9)$$

Let V_z be of the form $\exp(-ik_1x + ik_2y - i\eta t)$ times $\left\{A_1 \cosh(\tilde{k}z) + A_2 \sinh(\tilde{k}z)\right\}$. We note, however, that $A_1 = 0$ because a boundary condition requires that $V_z = 0$ at $z = 0$. Using this form for V_z in (A3.9) we find that

$$\tilde{k}^2\left(1 + \frac{igB_3^2}{\eta\rho}\right) = (k_1^2 + k_2^2)\left\{1 + \frac{ig}{\eta\rho}\frac{(B_1^2k_1^2 + B_2^2k_2^2)}{(k_1^2 + k_2^2)}\right\}. \qquad (A\,3.10)$$

The dispersion equation (relating η to k_1, k_2, $\tilde{k}$, B_0, H) is found by taking the time derivative of (6. 1. 4) and evaluating it at the surface. This gives

$$\rho\ddot{V}_z = -(\rho g + T[k_1^2 + k_2^2])\frac{\partial V_z}{\partial z} + g\left\{B_3(B_1V_x + B_2V_y + B_3V_z) - V_z(B_1^2 + B_2^2 + B_3^2)\right\}. \qquad (A\,3.11)$$

It is more convenient to consider two separate cases, I ($B_1 = 0 = B_2$) and II ($B_3 = 0$), when solving (A3.10) and (A3.11) simultaneously.

Case I ($B_1 = 0 = B_2$)

Using $V_z \propto \sinh(\tilde{k}z)e^{-i\eta t}$ we find that (A3.10) and (A3.11) reduce to

$$\left.\begin{aligned} \eta^2 &= [g + \tfrac{T}{\rho}(k_1^2 + k_2^2)]\tilde{k}\ \tanh(\tilde{k}H) \\ \tilde{k}^2\left(1 + \tfrac{igB_3^2}{\eta\rho}\right) &= k_1^2 + k_2^2 \\ \eta &= 2\pi f + i\sigma_B \\ \zeta &\propto \exp(ik_1x + ik_2y - i\eta t) \end{aligned}\right\} \qquad (A\,3.12)$$

For $B_3 = 0$ the above results agree with Coulson (ref. 6)

The problem of finding η in terms of k_1, k_2, H, and B_3 is simplified if we assume $\frac{gB_3^2}{\rho|\eta|} \ll 1$. Using this assumption and

using the fact that $\tanh\{A(1+i\theta)\} \simeq$

$$\{\tanh(A)\}\left\{1 + \frac{jA\theta 4}{(1+A^2\theta^2)(\exp(2A)-\exp(-2A))}\right\} \quad \text{FOR } \theta \ll 1$$

we find that (A 3.12) becomes

$$\left.\begin{aligned} n &= 2\pi f + i\sigma_B \\ (2\pi f)^2 &= \left\{\frac{Tk^3}{\rho} + gk\right\} TANH(kH) \\ \sigma_B &= -\frac{qB_3^2}{4\rho}\left\{1 + \frac{4kH}{\exp(2kH)-\exp(-2kH)}\right\} \\ k^2 &= k_1^2 + k_2^2 \\ \zeta &\propto \exp(ik_1x + ik_2y - int)\,. \end{aligned}\right\} \qquad (A\ 3.13)$$

The interesting points to note are the following:

(i) ζ is independent of B_3 for all values of kH.

(ii) σ_B is proportional to $\frac{qB_3^2}{\rho}$ for all kH.

(iii) $\sigma_B = -\frac{qB_3^2}{4\rho}$ for $kH \gg 1$. This result agrees with the theoretical calculation of Roberts and Boardman (ref. 26).

(iv) $\sigma_B = -\frac{qB_3^2}{2\rho}$ for $kH \ll 1$. This result agrees with the theoretical calculations of Fraenkel (ref. 24).

Case II ($B_3 = 0$)

Using $V_z \propto \sinh(\tilde{k}z)\,e^{-int}$ we find that (A 3.10) and (A 3.11) reduce to

$$\left.\begin{aligned} n^2 &= \left\{g + \frac{T}{\rho}(k_1^2+k_2^2)\right\}\tilde{k}\,TANH(\tilde{k}H) - \frac{in}{\rho}q(B_1^2+B_2^2) \\ \tilde{k}^2 &= \left\{k_1^2+k_2^2\right\}\left\{1 + iq\frac{(B_1^2k_1^2 + B_2^2k_2^2)}{n\rho(k_1^2+k_2^2)}\right\} \\ n &= 2\pi f + i\sigma_B\,. \end{aligned}\right\} \qquad (A\ 3.14)$$

Again the problem of finding n in terms of k_1 , k_2 , H, B_1 and B_2 is simplified if we assume $\frac{q(B_1^2+B_2^2)}{\rho|n|} \ll 1$. Using this assumption

and using the fact that $\tanh\{A(1+i\Theta)\} \simeq$

$$\{TANH(A)\}\left\{1 + \frac{i4A\Theta}{(1+A^2\Theta^2)(EXP(2A)-EXP(-2A))}\right\} \quad FOR\ \Theta \ll 1$$

we find that (A3.14) reduces to

$$\left.\begin{aligned} &n = 2\pi f + i\sigma_B \\ &(2\pi f)^2 = \left\{\frac{Tk^3}{\rho} + gk\right\} TANH(kH) \\ &\sigma_B = -\frac{q}{4\rho}\left\{2(B_1^2+B_2^2) - \frac{(B_1^2k_1^2 + B_2^2k_2^2)}{k_1^2+k_2^2}\left(1 + \frac{4kH}{EXP(2kH)-EXP(-2kH)}\right)\right\} \\ &k^2 = k_1^2 + k_2^2 \\ &\xi \propto EXP(ik_1x + ik_2y - int). \end{aligned}\right\} \quad (A3.15)$$

The interesting points to note are the following:

(i) f is independent of B_1 and B_2 for all kH.

(ii) $\sigma_B \simeq -\frac{q}{4\rho}\left\{2(B_1^2+B_2^2) - \frac{B_1^2k_1^2 + B_2^2k_2^2}{k_1^2+k_2^2}\right\}$ FOR $kH \gg 1$.

For the case $B_2 = k_2 = 0$ this agrees with the theoretical calculations of Wentzell and Blackwell (ref. 27) and also Kukshas et al. (ref. 28).

(iii) $\sigma_B \simeq -\frac{q}{4\rho}\left\{2(B_1^2+B_2^2) - \frac{(B_1^2k_1^2 + B_2^2k_2^2)}{k_1^2+k_2^2}\left(2 - \frac{2}{3}(kH)^2\right)\right\}$ FOR $kH \ll 1$.

For the case $B_2 = 0 = k_2$ this agrees with Kukshas et al.

Kukshas et al. claim that $\sigma_B \simeq 0$ if $k_2 = 0$ and $B_1 = 0$ or if $k_1 = 0$ and $B_2 = 0$ (i.e. if the applied magnetic field is parallel to the wave front). This claim does not agree with our calculations.

The problem of solving (A3.12) and (A3.14) for all values of $\frac{q(B_1^2+B_2^2+B_3^2)}{\rho|n|}$ was not considered.

APPENDIX 4 MUMMERY SUMMARY

The following is based on work by F. Winsor (ref. 45).

This is the theory Jack built.

This is the flaw
that lay in the theory Jack built.

This is the mummery
hiding the flaw
that lay in the theory Jack built.

This is the summary
based on the mummery
hiding the flaw
that lay in the theory Jack built.

This is the constant K
that saved the summary
based on the mummery
hiding the flaw
that lay in the theory Jack built.

This is the erudite verbal haze
cloaking constant K
that saved the summary
based on the mummery
hiding the flaw
that lay in the theory Jack built.

This is the turn of a plausible phrase
that thickened the erudite verbal haze
cloaking constant K
that saved the summary
based on the mummery
hiding the flaw
that lay in the theory Jack built.

This is chaotic confusion and bluff
that hung on the turn of a plausible phrase
that thickened the erudite verbal haze
cloaking constant K
that saved the summary
based on the mummery
hiding the flaw
that lay in the theory Jack built.

This is the electromagnetics and stuff
that covered chaotic confusion and bluff
that hung on the turn of a plausible phrase
and thickened the erudite verbal haze
cloaking constant K
that saved the summary
based on the mummery
hiding the flaw
that lay in the theory Jack built.

This is the microwave cavity machine
to make with the electromagnetics and stuff
to cover chaotic confusion and bluff
that hung on the turn of a plausible phrase
and thickened the erudite verbal haze
cloaking constant K
that saved the summary
based on the mummery
hiding the flaw
that lay in the theory Jack built.

This is the fool with brow serene
who started the microwave cavity machine
that made with the electromagnetics and stuff
without confusion, exposing the bluff
that hung on the turn of a plausible phrase
and, shredding the erudite verbal haze,
cloaking constant K
wrecked the summary
based on the mummery
hiding the flaw
and demolished the theory Jack built.

This is the theory Rob built.

This is the flaw
that lay in the theory Rob built .....